

Electronic supporting information

Nickel(II) complexes containing tridentate ONC^i Ligands ($i = \text{abnormal } N\text{-heterocyclic carbene}$ donors) and their catalytic application in Suzuki-Miyaura coupling reaction

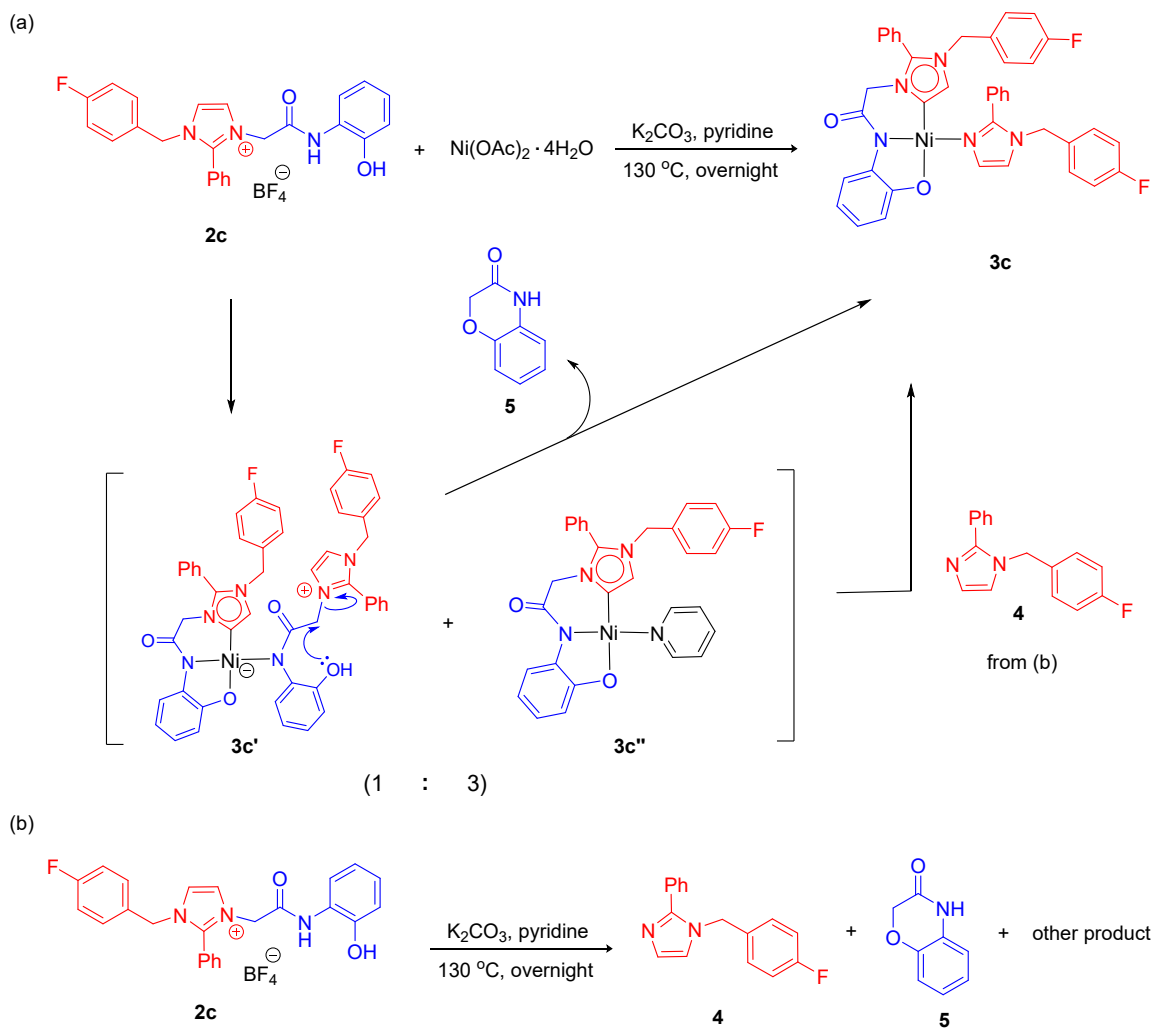
Jhen-Yi Lee, Meng-Jun Hsieh, Tsai-En Ho, Bo-Hsin Wu and Hon Man Lee*

Department of Chemistry, National Changhua University of Education, Changhua 50058, Taiwan.

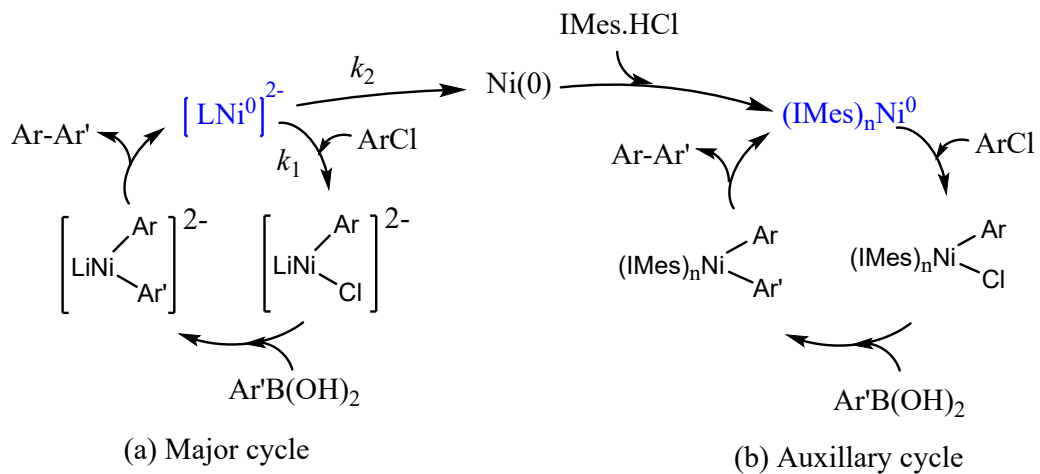
leehm@cc.ncue.edu.tw

Table of contents

1. Schemes and additional discussion	S2
2. Procedure for X-ray structural studies	S3
3. Crystallographic data	S4
4. Atom connectivity in 3c	S5
5. Time-conversion profiles	S5
6. ^1H and $^{13}\text{C}\{^1\text{H}\}$ NMR spectra of ligand precursors and nickel complexes	S6
7. 2D HMBC spectra of nickel complexes	S14
8. ^1H NMR data of catalytic products	S17
9. ^1H NMR spectra of catalytic products	S20
10. Mass spectra	S29
11. References	S31



Scheme S1. Mechanistic pathway for the formation of **3c**.



Scheme S2. A speculative catalytic cycle for the Suzuki-Miyaura coupling reaction catalyzed by

3b/IMes·HCl.

Generally, the reaction proceeds via a classical catalytic cycle of Suzuki-Miyaura coupling reaction involving the O,N,C-chelated Ni(0) active species. Then an oxidative addition of the aryl chloride substrate occurs, forming the Ar—Ni(II) intermediate. Transmetalation of the aryl group from the boron to the nickel center led to the diaryl intermediate. An aryl group bearing an electron-withdrawing group enhances its transfer on the nickel center, whereas an aryl group with an electron-donating group disfavors the process. The diaryl intermediate then undergoes a reductive elimination to give the couple product. The oxidative addition step is most probably the r.d.s of the catalytic cycle. However, a small amount of the O,N,C-chelated Ni(0) active species can also undergo a catalyst degradation to form off-loop homogeneous ligand-free Ni(0) or heterogeneous Ni(0) nanoparticles (See entry 8 in Table 3). The in situ formed IMes ligand from the IMes·HCl additive is able to capture these Ni(0) species to form $\text{Ni}^0(\text{IMes})$, which can then catalyze the formation of the couple product in an auxiliary cycle. For activated aryl chloride substrate, the oxidative addition step is much faster than the degradation step (rate constant $k_1 \gg k_2$) and thus the product yield enhancement is low ($\text{CF}_3 = 1.7$). But in the case of de-activated substrates, the oxidative addition step becomes slower. Hence, more Ni(0) species enters the auxiliary cycle such that higher product enhancement ratios were observed ($\text{OMe} = 3.7$).

Single-crystal X-ray diffraction. Structural data of **3b** **3c**, and **3c''** were collected on a Bruker SMART APEX II equipped with a CCD area detector. Data collection were carried out at 150(2) K

using MoK α radiation ($\lambda = 0.71073 \text{ \AA}$). The unit cell parameters were obtained by least-squares refinement. Data collection and reduction were performed using the Bruker APEX and SAINT software.¹ Absorption corrections were performed using the SADABS program.² All the structures were solved by direct methods and refined by full-matrix least squares methods against F^2 with the SHELXL software package.³ All non-hydrogen atoms were refined in anisotropic manners. All hydrogen atoms were positioned at calculated positions and riding refinements were then applied. The structure of **3b** was refined as a non-merohedral twin. The structure of **3c** contains disordered DMF solvent molecules and their structural factor contributions were removed by the SQUEEZE procedure.⁴ CCDC files numbers: 2100759 (**3b**), 2100760 (**3c''**), and 2100761 (**3c**).

Table S1. Crystallographic data

	3b	3c''	3c
empirical formula	C ₄₂ H ₃₇ N ₅ NiO ₄ ·CH ₂ Cl ₂	C ₂₉ H ₂₃ FN ₄ NiO ₂	C ₄₀ H ₃₁ F ₂ N ₅ NiO ₂
formula weight	819.38	537.22	710.41
crystal system	monoclinic	monoclinic	Monoclinic
space group	<i>P</i> 2 ₁ / <i>c</i>	<i>P</i> 2 ₁ / <i>c</i>	<i>P</i> 2 ₁ / <i>n</i>
<i>a</i> , Å	16.621(3)	10.403(6)	9.003(4)
<i>b</i> , Å	11.825(2)	27.246(14)	15.252(6)
<i>c</i> , Å	20.184(4)	8.775(5)	30.153(12)
α , deg	90	90	90
β , deg	99.400(4)	102.236(15)	96.36(3)
γ , deg	90	90	90
<i>V</i> , Å ³	3913.9(13)	2431(2)	4115(3)
<i>T</i> , K	150(2)	150(2)	150
<i>Z</i>	4	4	4
F(000)	1704	1112	1472
no. of unique data	8523	5023	8526
no. of params refined	527	335	452
<i>R</i> ₁ ^a [<i>I</i> > 2σ <i>I</i>]	0.0467	0.0623	0.1242
<i>wR</i> ₂ ^b (all data)	0.1393	0.1377	0.3032

^a*R*₁ = Σ(|*F*_o| - |*F*_c|)/Σ|*F*_o|. ^b *wR*₂ = [Σ(|*F*_o|² - |*F*_c|²)²/Σ(*F*_o²)]^{1/2}

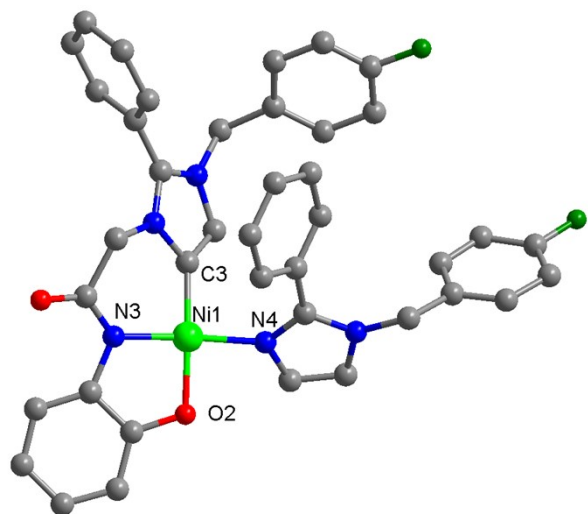


Figure S1. Low-resolution structural data showing the atom connectivity in **3c**.

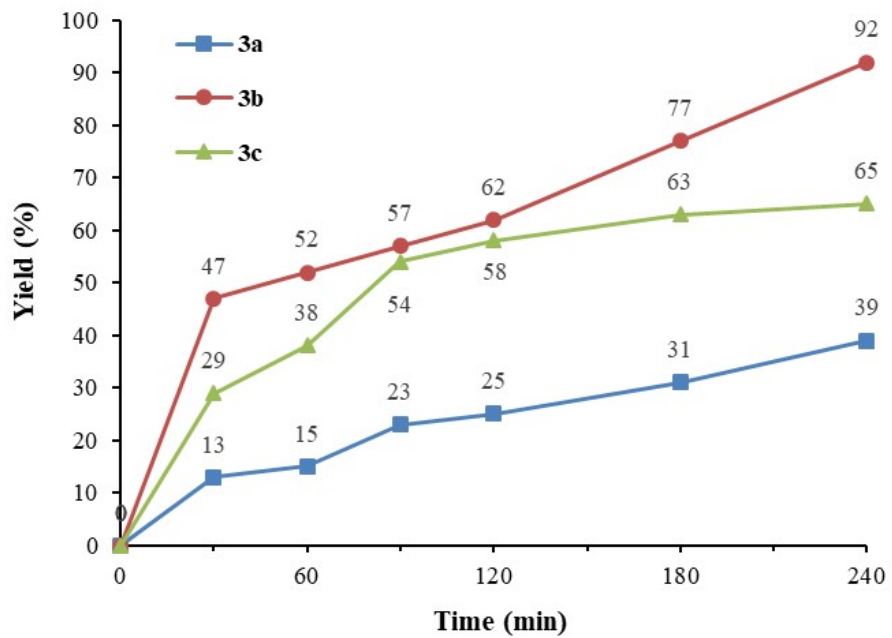


Figure S2. The time-conversion profiles for the reaction between 4-chloroacetophenone and phenylboronic acid catalyzed by **3a-c**.

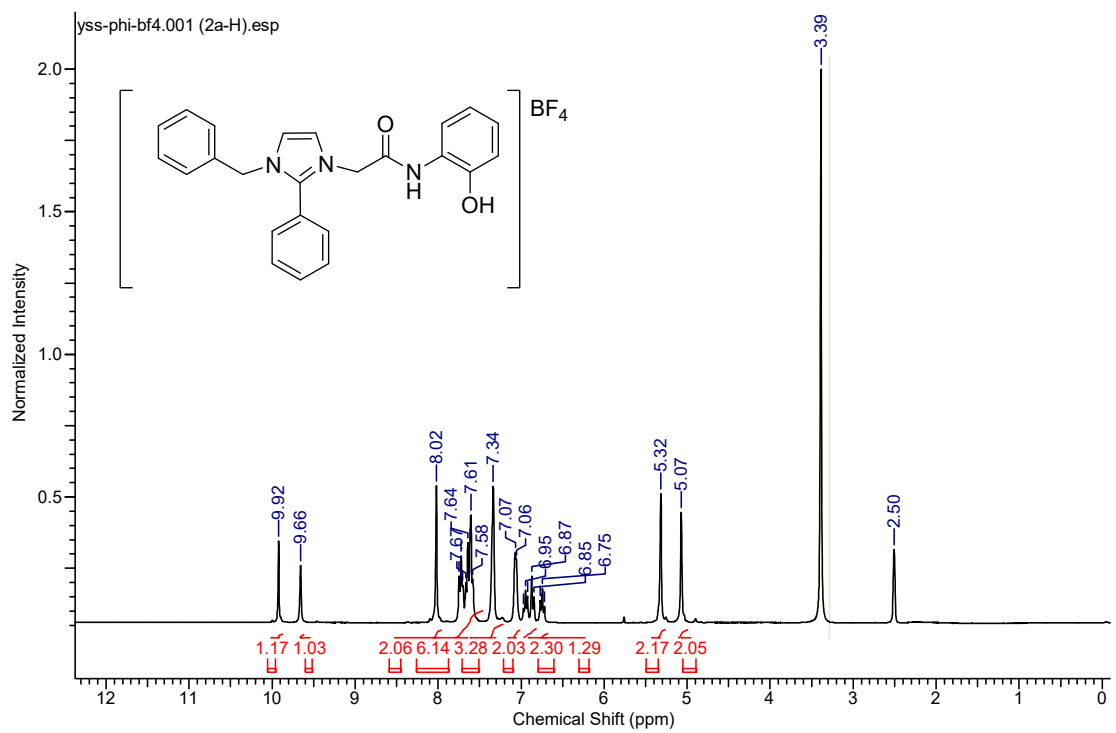


Figure S3. ^1H NMR spectrum of **2a**

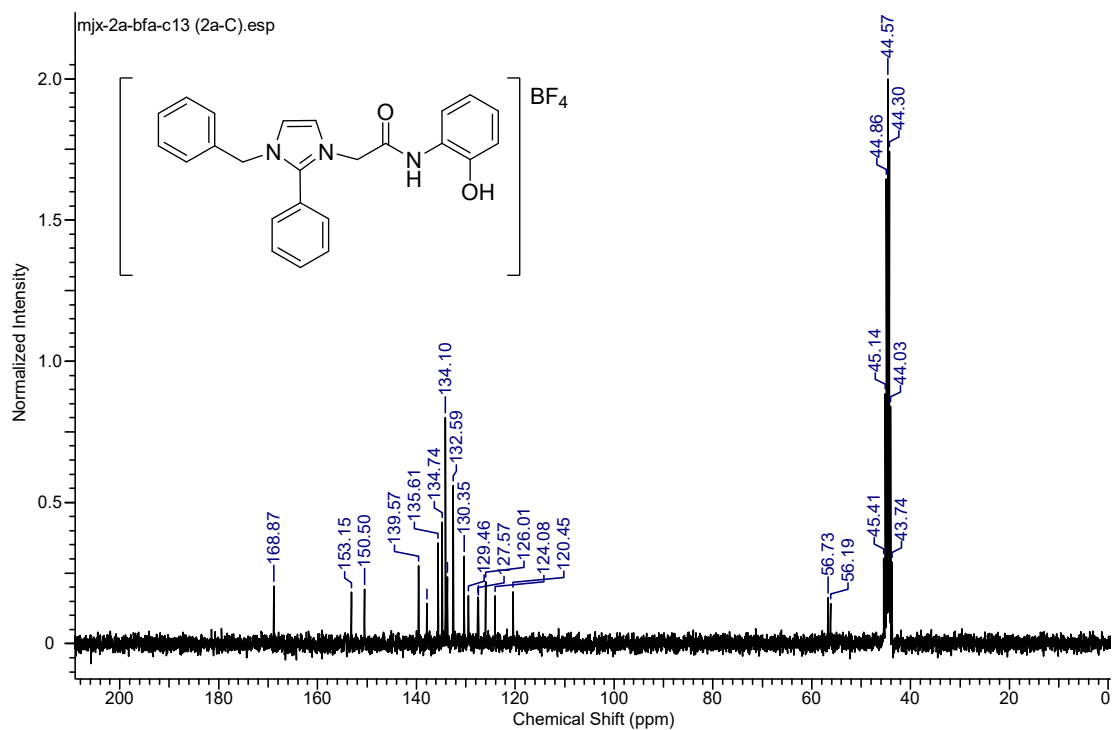


Figure S4. $^{13}\text{C}\{^1\text{H}\}$ NMR spectrum of **2a**

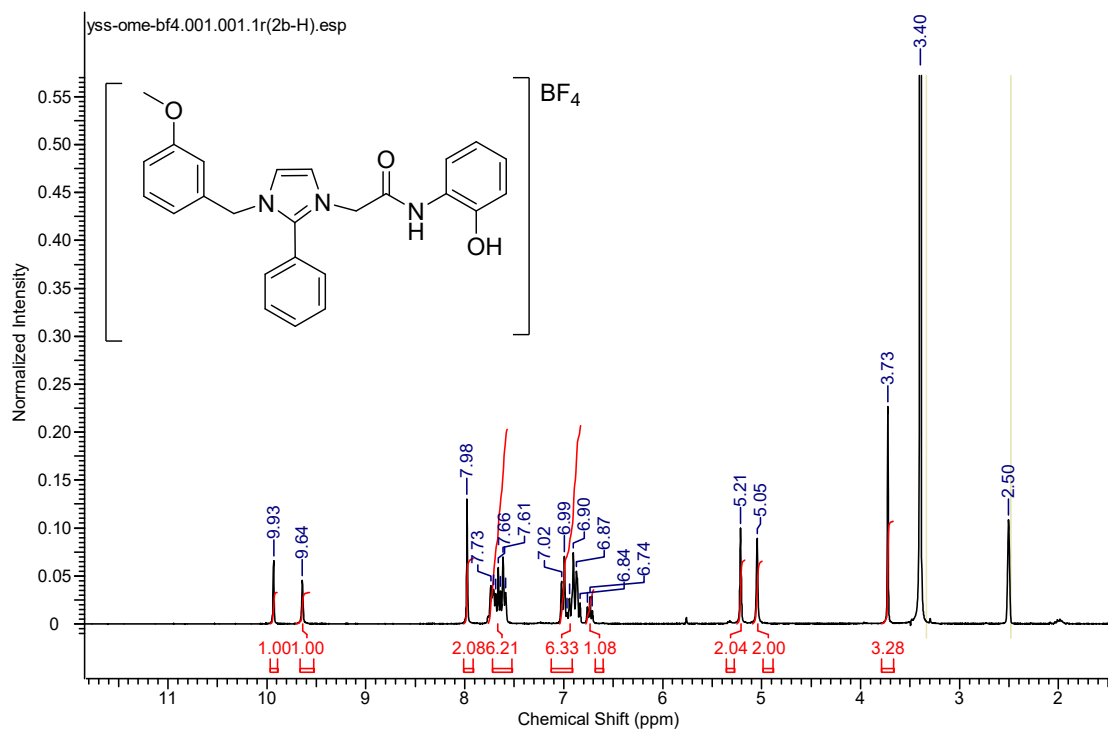


Figure S5. ^1H NMR spectrum of **2b**

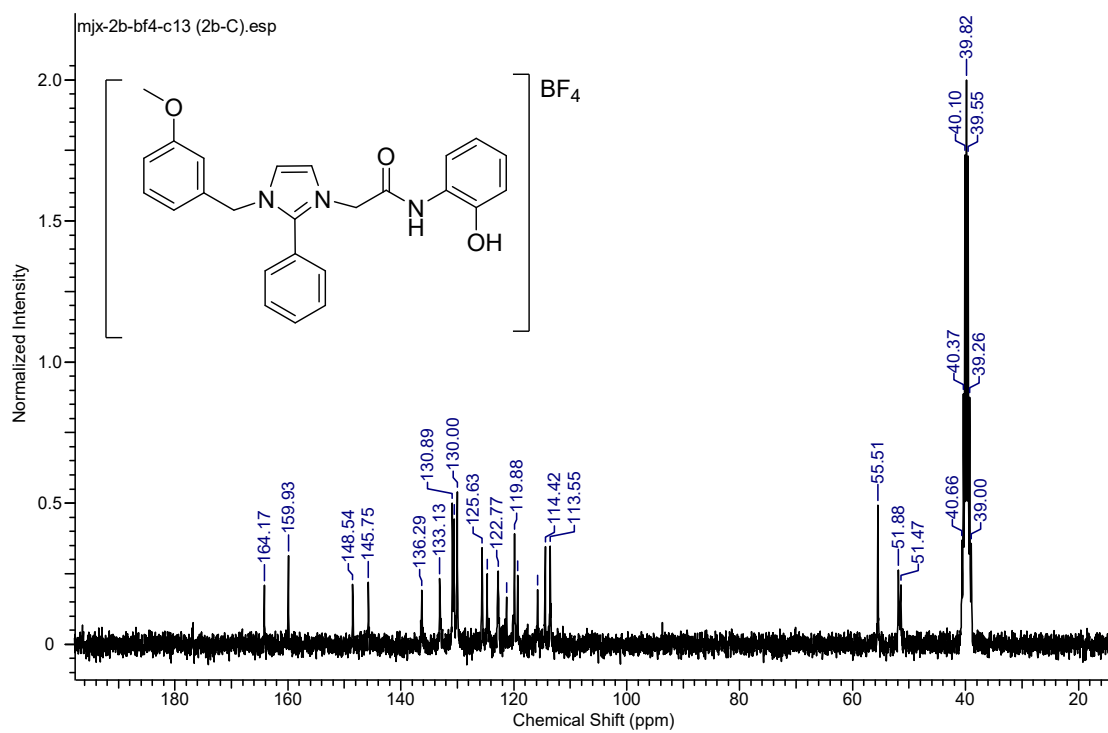


Figure S6. $^{13}\text{C}\{^1\text{H}\}$ NMR spectrum of **2b**

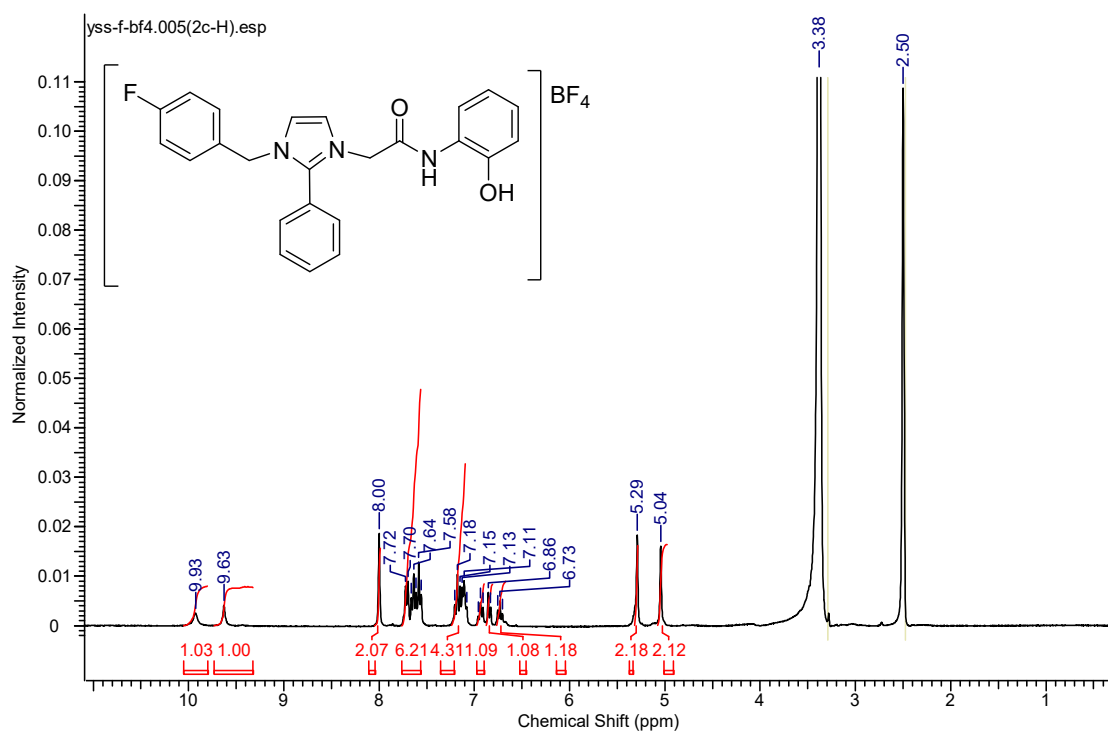


Figure S7. ^1H NMR spectrum of **2c**

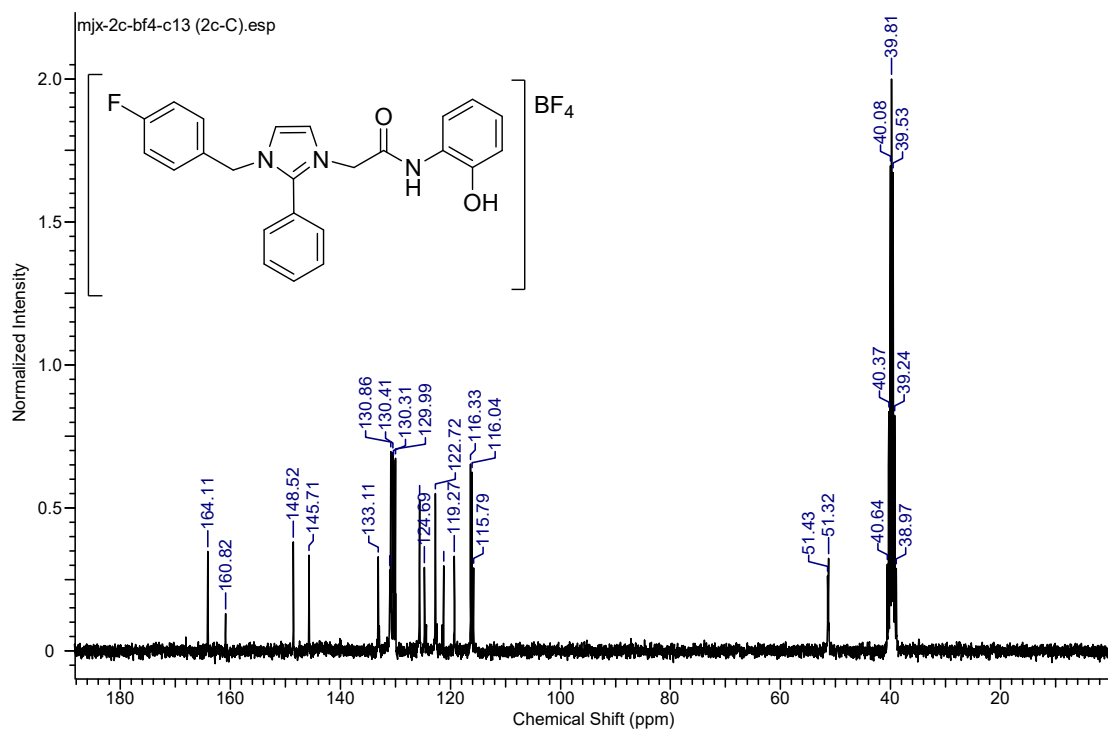


Figure S8. $^{13}\text{C}\{^1\text{H}\}$ NMR spectrum of **2c**

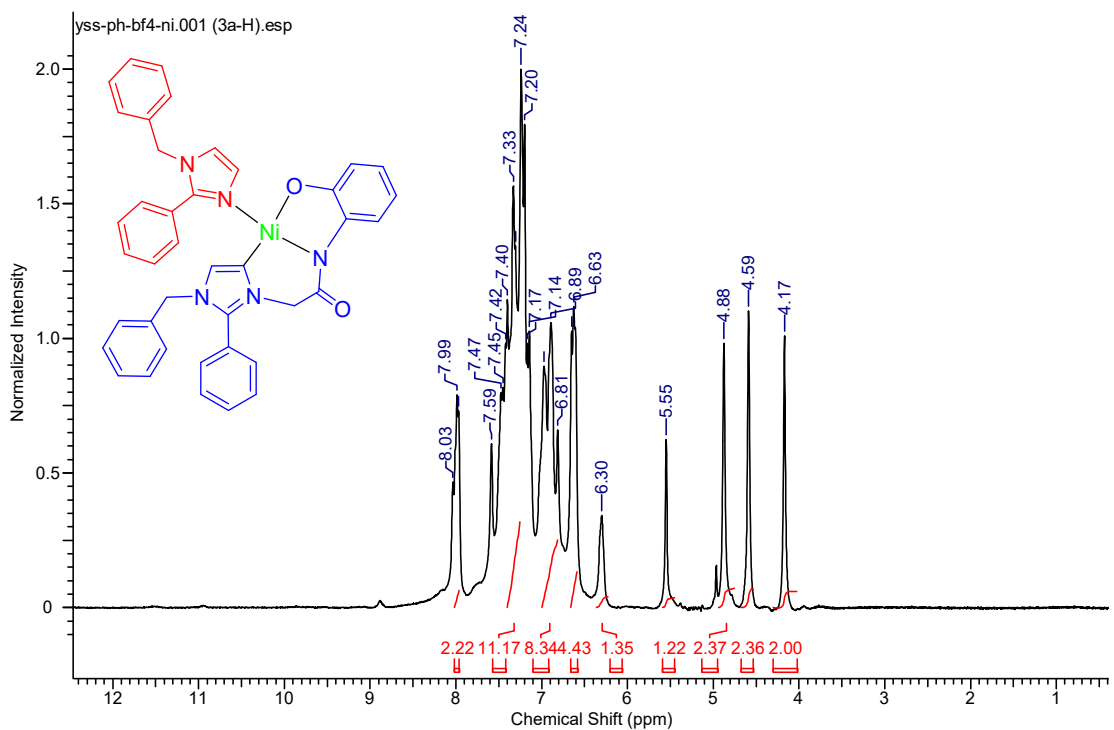


Figure S9. ^1H NMR spectrum of **3a**

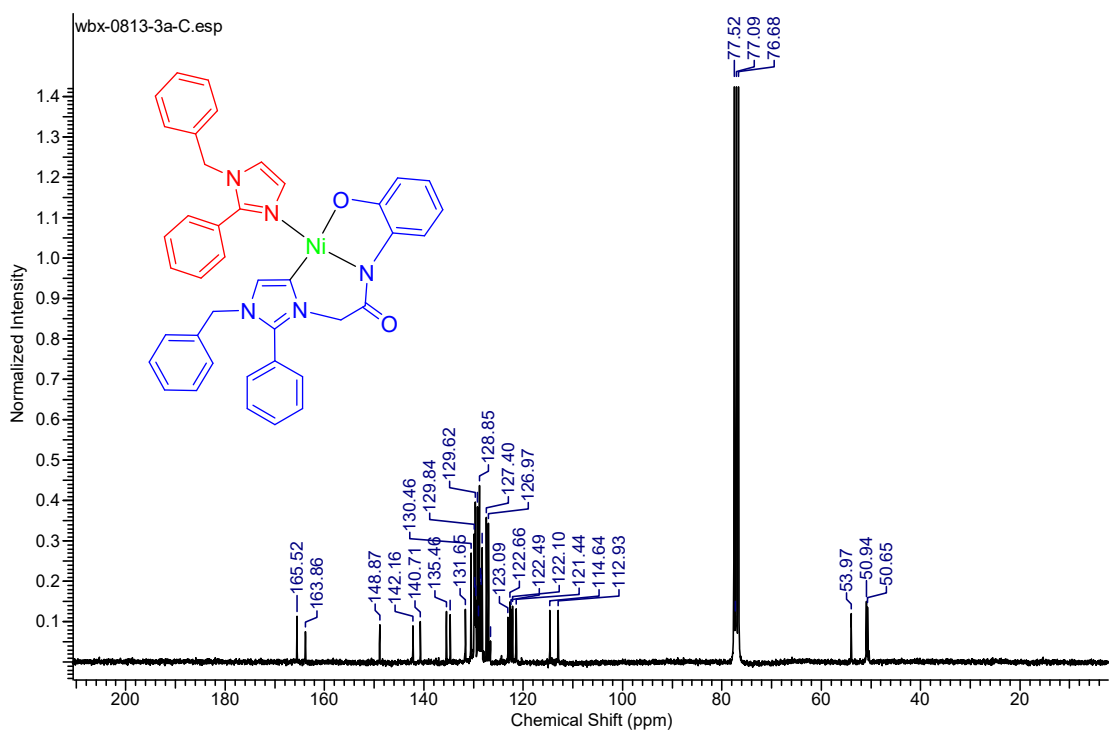


Figure S10. $^{13}\text{C}\{\text{H}\}$ NMR spectrum of **3a**

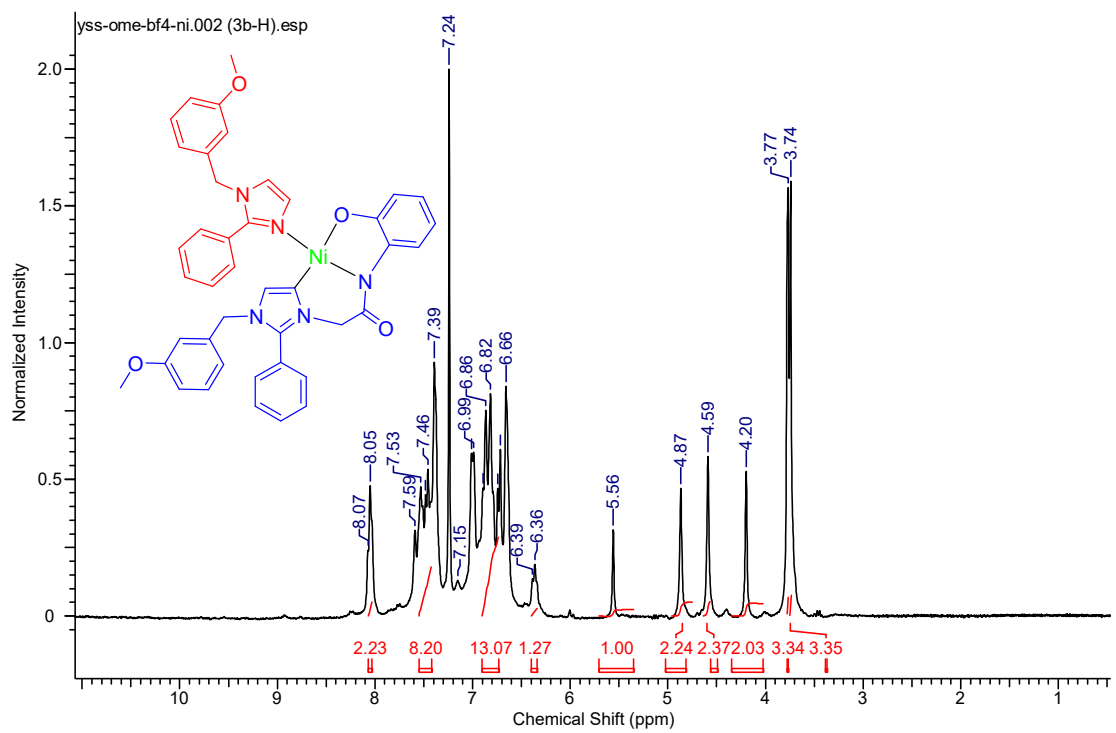


Figure S11. ^1H NMR spectrum of **3b**

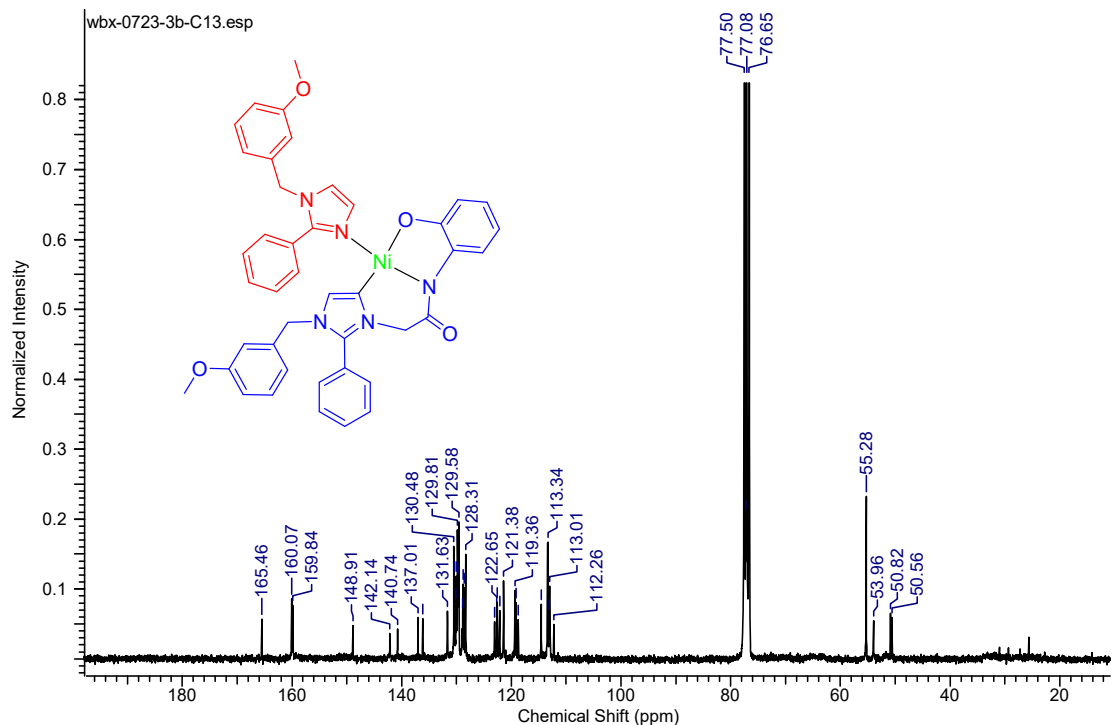


Figure S12. $^{13}\text{C}\{\text{H}\}$ NMR spectrum of **3b**

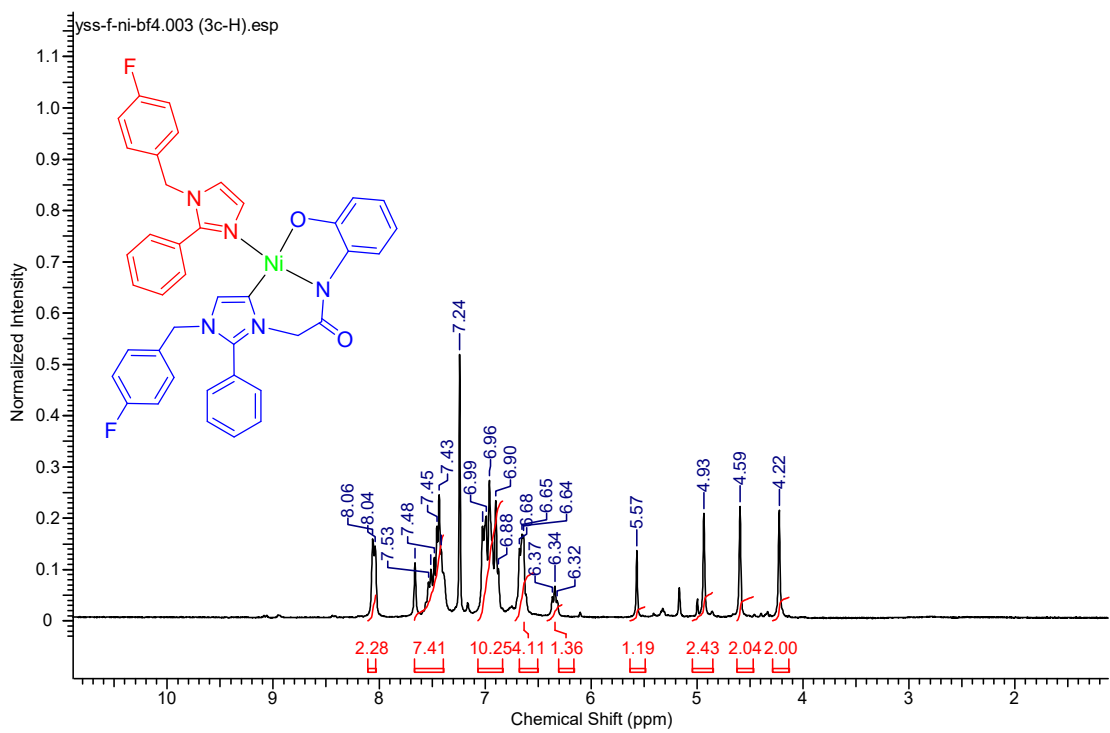


Figure S13. ^1H NMR spectrum of **3c**

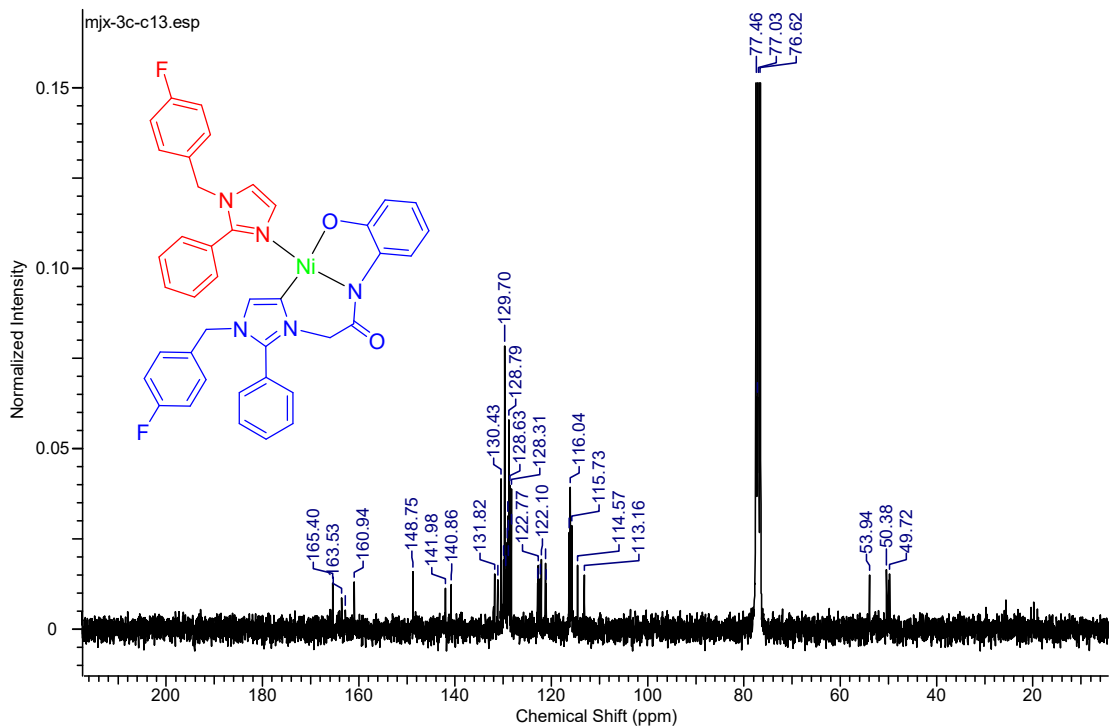


Figure S14. $^{13}\text{C}\{^1\text{H}\}$ NMR spectrum of **3c**

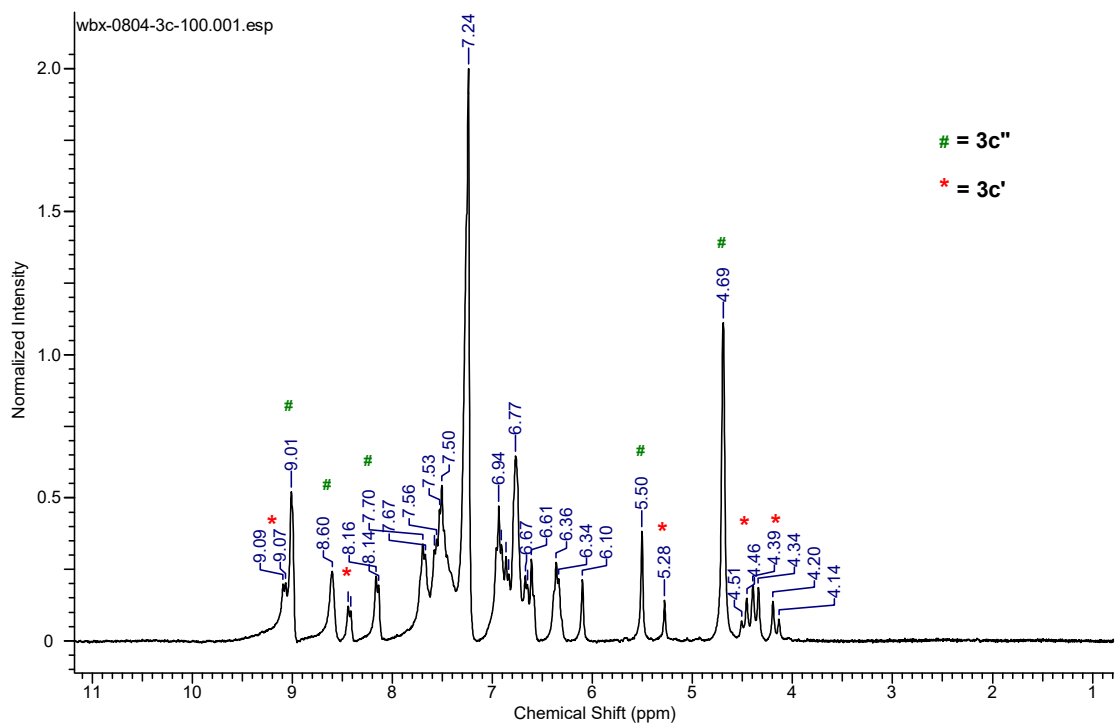


Figure S15. The ^1H NMR spectrum of a mixture of complexes $\mathbf{3c}'$ and $\mathbf{3c}''$.

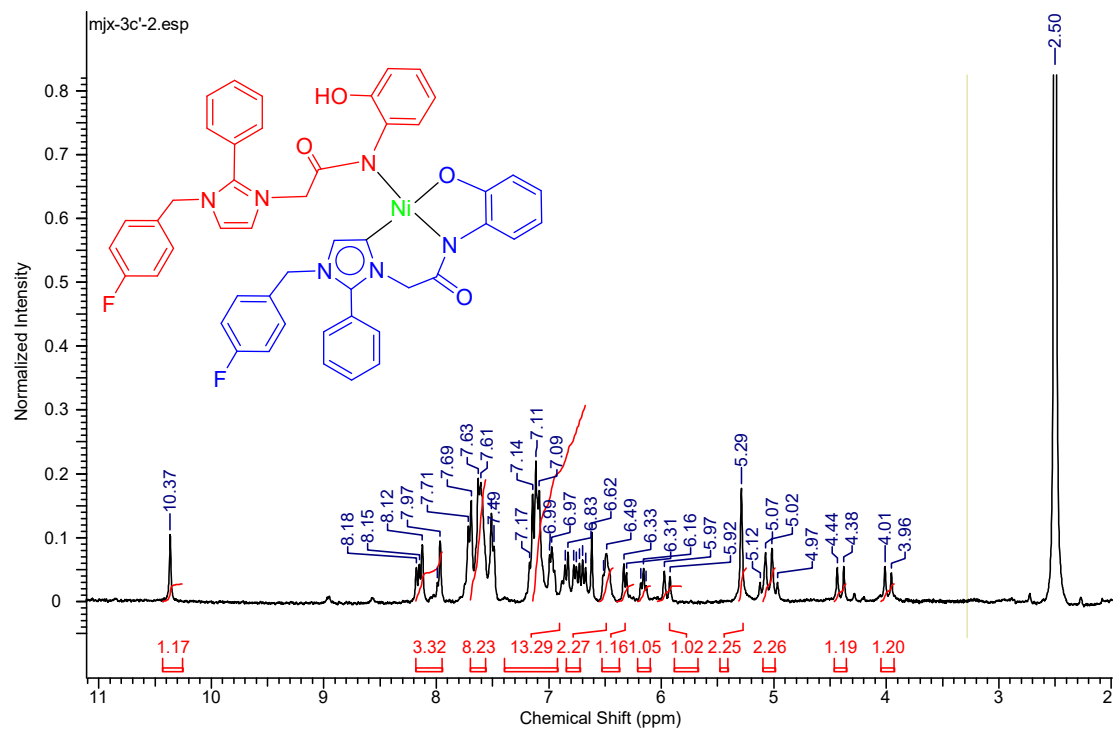


Figure S16. ^1H NMR spectrum of $\mathbf{3c}'$

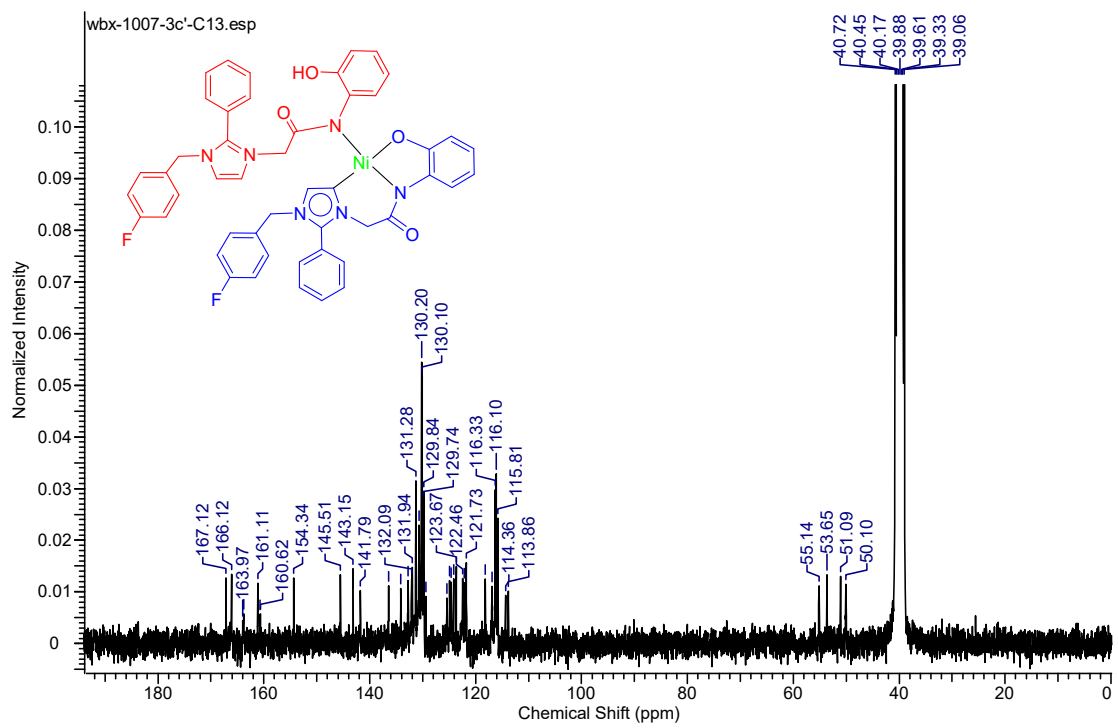


Figure S17. $^{13}\text{C}\{\text{H}\}$ NMR spectrum of $3\text{c}'$

MJX3A-HMBC.001.001.2r.esp

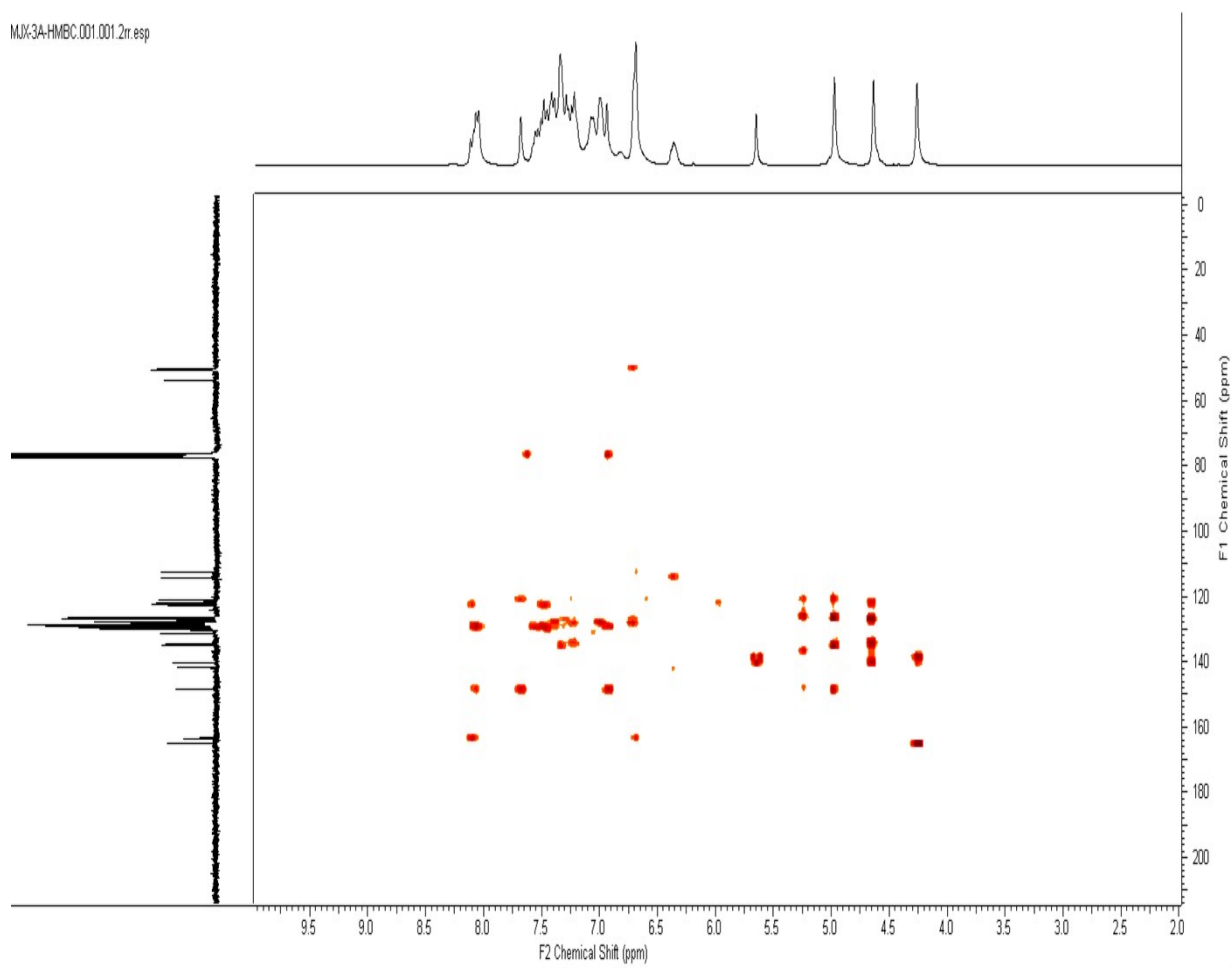


Figure S18. HMBC spectrum of **3a**

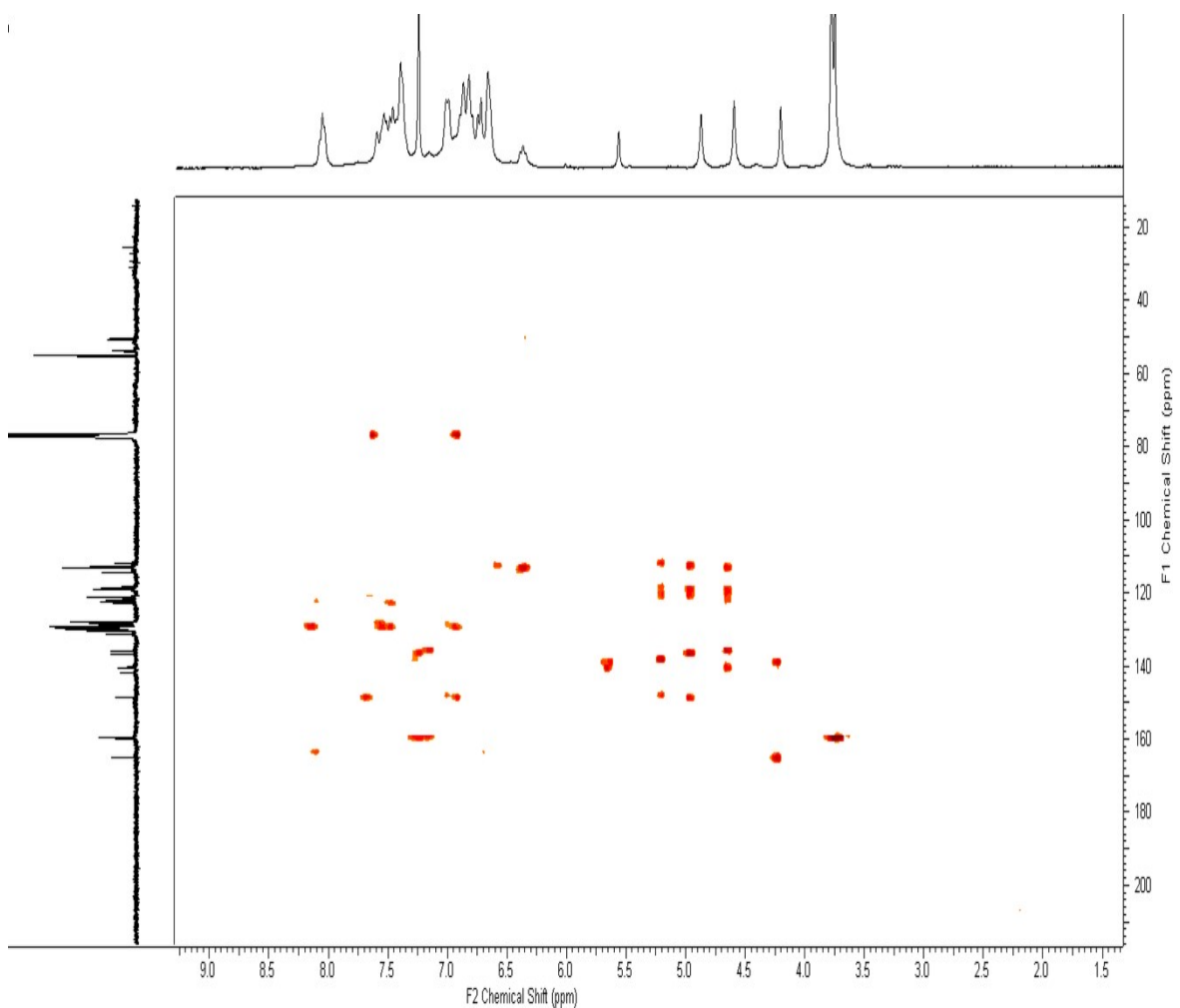


Figure S19. HMBC spectrum of **3b**

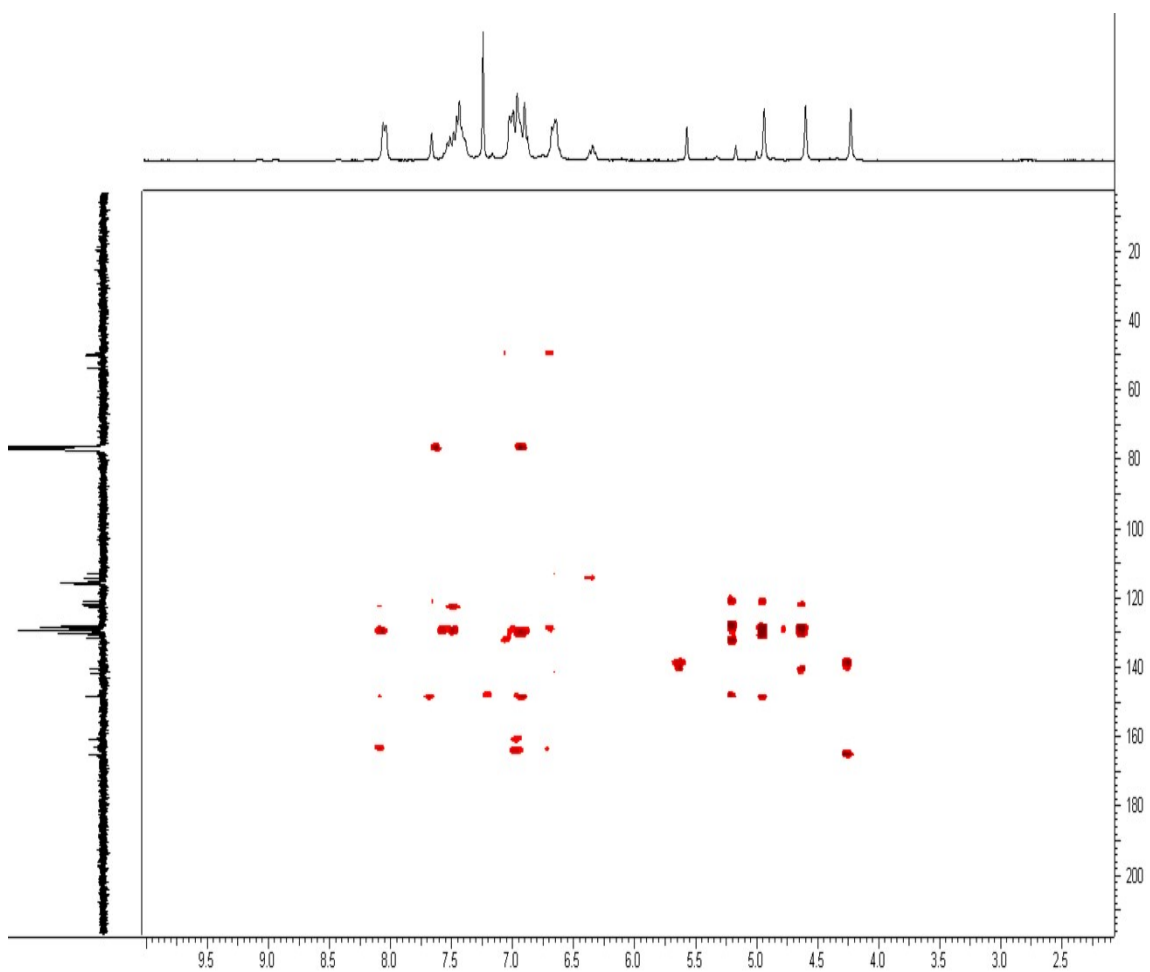


Figure S20. HMBC spectrum of **3c**

¹H NMR Data of Catalytic Products

4-Acetyl biphenyl⁵ (6): ¹H NMR (CDCl₃): δ 2.63 (s, 3H, CH₃), 7.39-7.49 (m, 3H, Ar H), 7.61-7.69 (m, 4H, Ar H), 8.03 (d, *J* = 9.0 Hz, 2H, Ar H).

3-Acetyl biphenyl⁶ (6'): ¹H NMR (CDCl₃): δ 2.59 (s, 3H, CH₃), 7.33 (t, *J* = 6.0 Hz, 1H, Ar H), 7.39-7.48 (m, 3H, Ar H), 7.57 (d, *J* = 9.0 Hz, 2H, Ar H), 7.72 (d, *J* = 9.0 Hz, 1H, Ar H), 7.88 (d, *J* = 9.0 Hz, 1H, Ar H), 8.15 (s, 1H, Ar H).

4-(Trifluoromethyl)-1,1'-biphenyl⁷ (7): ¹H NMR (CDCl₃): δ 7.39-7.48 (m, 3H, Ar H), 7.58 (d, *J* = 6.0 Hz, 2H, Ar H), 7.68 (br s, 4H, Ar H).

4-Phenylbenzaldehyde⁶ (8): ¹H NMR (CDCl₃): δ 7.40-7.49 (m, 3H, Ar H), 7.61 (d, *J* = 6.0 Hz, 2H, Ar H), 7.72 (d, *J* = 9.0 Hz, 2H, Ar H), 7.92 (d, *J* = 6.0 Hz, 2H, Ar H), 10.02 (s, 1H, O=CH).

[1,1'-Biphenyl]-4-carbonitrile⁶ (9): ¹H NMR (CDCl₃): δ 7.41-7.49 (m, 3H, Ar H), 7.57 (d, *J* = 6.0 Hz, 2H, Ar H), 7.65-7.73 (m, 4H, Ar H).

4-Methoxy-1,1'-biphenyl⁵ (10): ¹H NMR (CDCl₃): δ 3.84 (s, 3H, OCH₃), 6.97 (d, *J* = 9.0 Hz, 2H, Ar H), 7.29 (t, *J* = 6.0 Hz, 1H, Ar H), 7.40 (t, *J* = 9.0 Hz, 2H, Ar H), 7.50-7.55 (m, 4H, Ar H).

1-(4'-Fluoro-[1,1'-biphenyl]-4-yl)ethanone⁵ (11): ¹H NMR (CDCl₃): δ 2.60 (s, 3H, CH₃), 7.12 (t, *J* = 6.0 Hz, 2H, Ar H), 7.53-7.60 (m, 4H, Ar H), 7.99 (d, *J* = 9.0 Hz, 2H, Ar H).

4-Fluoro-4'-(trifluoromethyl)-1,1'-biphenyl⁸ (12): ¹H NMR (CDCl₃): δ 7.08-7.18 (m, 2H, Ar H), 7.37-7.69 (m, 6H, Ar H).

4'-Fluoro-[1,1'-biphenyl]-4-carbaldehyde⁵ (13): ¹H NMR (CDCl₃): δ 7.15 (t, *J* = 9.0 Hz, 2H, Ar H),

7.57-7.61 (m, 2H, Ar H), 7.69 (d, J = 6.0 Hz, 2H, Ar H), 7.94 (d, J = 9.0 Hz, 2H, Ar H), 10.04 (s, 1H, O=CH).

4'-Fluoro-[1,1'-biphenyl]-2-carbaldehyde⁹ (13'): ^1H NMR (CDCl_3): δ 7.13 (t, J = 9.0 Hz, 2H, Ar H), 7.29-7.39 (m, 3H, Ar H), 7.46 (t, J = 9.0 Hz, 1H, Ar H), 7.60 (t, J = 9.0 Hz, 1H, Ar H), 7.99 (d, J = 9.0 Hz, 1H, Ar H), 9.93 (s, 1H, O=C-H).

4-Fluoro-4'-methoxybiphenyl⁸ (14): ^1H NMR (CDCl_3): δ 3.83 (s, 3H, CH_3), 6.96 (d, J = 9.0 Hz, 2H, Ar H), 7.08 (t, J = 9.0 Hz, 2H, Ar H), 7.44-7.50 (m, 4H, Ar H).

1-(4'-Methoxy-[1,1'-biphenyl]-4-yl)ethanone⁵ (15): ^1H NMR (CDCl_3): δ 2.61 (s, 3H, O= C- CH_3), 3.85 (s, 3H, OCH_3), 6.99 (d, J = 9.0 Hz, 2H, Ar H), 7.57 (d, J = 9.0 Hz, 2H, Ar H), 7.63 (d, J = 6.0 Hz, 2H, Ar H), 8.00 (d, J = 9.0 Hz, 2H, Ar H).

4-Methoxy-4'-(trifluoromethyl)-1,1'-biphenyl⁵ (16): ^1H NMR (CDCl_3): δ 3.85 (s, 3H, OCH_3), 6.93-7.00 (m, 2H, Ar H), 7.45-7.54 (m, 2H, Ar H), 7.64 (br s, 4H, Ar H).

4'-Methoxy-[1,1'-biphenyl]-4-carbaldehyde⁵ (17): ^1H NMR (CDCl_3): δ 3.84 (s, 3H, OCH_3), 6.99 (d, J = 9.0 Hz, 2H, Ar H), 7.57 (d, J = 9.0 Hz, 2H, Ar H), 7.68 (d, J = 6.0 Hz, 2H, Ar H), 7.89 (d, J = 6.0 Hz, 2H, Ar H), 10.00 (s, 1H, O=C-H).

4,4'-Dimethoxy-1,1'-biphenyl¹⁰ (18): ^1H NMR (CDCl_3): δ 3.83 (s, 6H, CH_3), 6.95 (d, J = 9.0 Hz, 4H, Ar H), 7.46 (d, J = 9.0 Hz, 4H, Ar H).

1-(4-(Naphthalen-1-yl)phenyl)ethanone¹¹ (19): ^1H NMR (CDCl_3): δ 2.66 (s, 3H, CH_3), 7.40-7.59 (m, 6H, Ar H), 7.88-7.93 (m, 3H, Ar H), 8.08 (d, J = 9.0 Hz, 2H, Ar H).

1-(4-(Trifluoromethyl)phenyl)naphthalene⁸ (20): ^1H NMR (CDCl_3): δ 7.47-7.68 (m, 5H, Ar H),

7.85 (d, J = 9.0 Hz, 2H, Ar H), 7.92-8.03 (m, 4H, Ar H).

4-(Naphthalen-1-yl)benzaldehyde¹² (21): ^1H NMR (CDCl_3): δ 7.41-7.57 (m, 4H, Ar H), 7.66 (d, J = 6.0 Hz, 2H, Ar H), 7.84 (d, J = 9.0 Hz, 1H, Ar H), 7.91 (t, J = 9.0 Hz, 2H, Ar H), 8.00 (d, J = 9.0 Hz, 2H, Ar H), 10.10 (s, 1H, O=C-H).

1-(4-(Benzofuran-2-yl)phenyl)ethan-1-one¹³ (23): ^1H NMR (CDCl_3): δ 2.61 (s, 3H, CH_3), 7.14 (s, 1H, Ar-H), 7.24 (t, J = 6.0 Hz, 1H, Ar H), 7.32 (t, J = 6.0 Hz, 1H, Ar H), 7.53 (d, J = 9.0 Hz, 1H, Ar H), 7.60 (d, J = 9.0 Hz, 1H, Ar H), 7.92 (d, J = 9.0 Hz, 2H, Ar H), 8.02 (d, J = 9.0 Hz, 2H, Ar H).

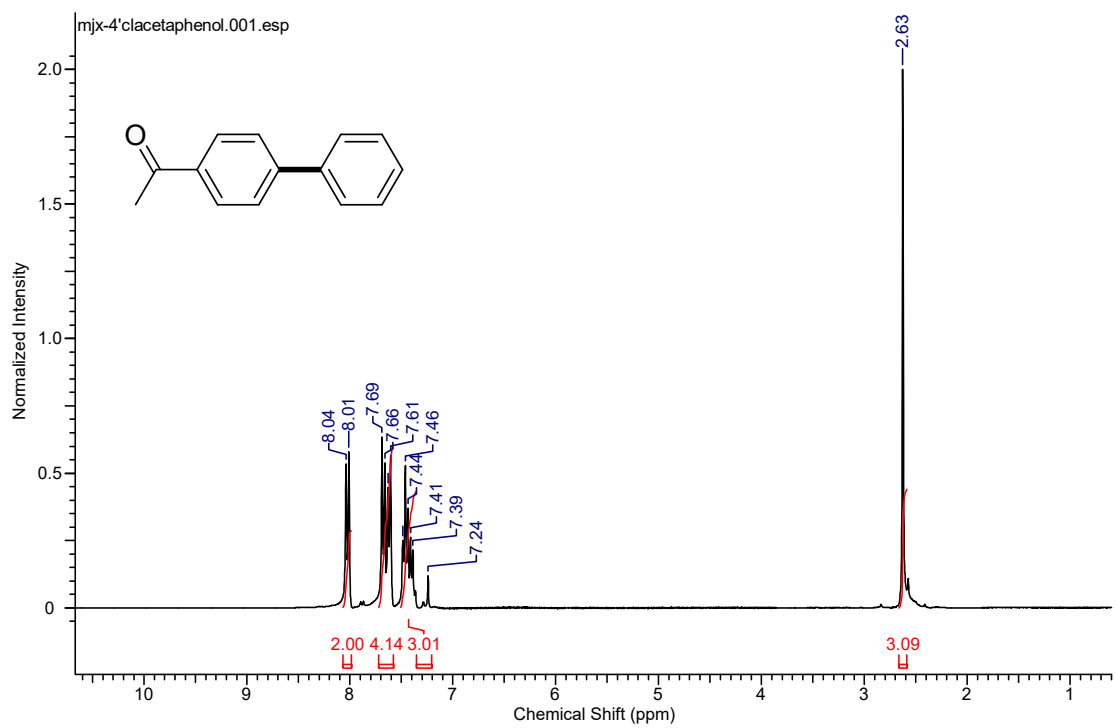


Figure S21. ^1H NMR spectrum of 4-acetyl biphenyl (**6**)

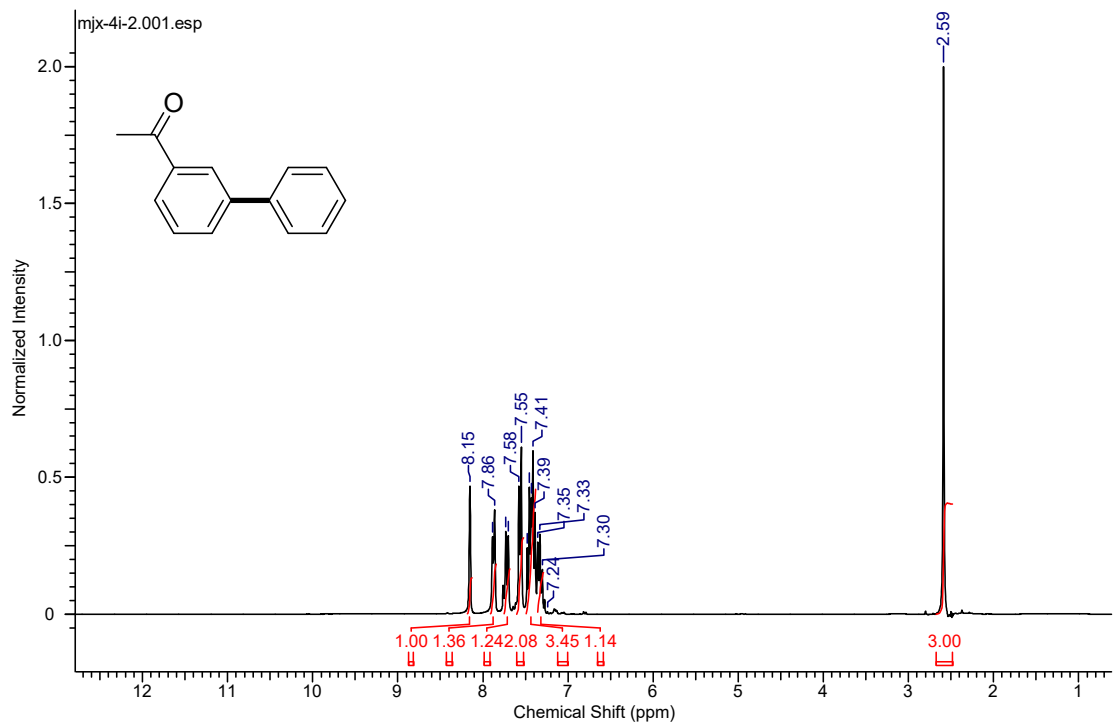


Figure S22. ^1H NMR spectrum of 1-([1,1'-biphenyl]-3-yl)ethanone (**6'**)

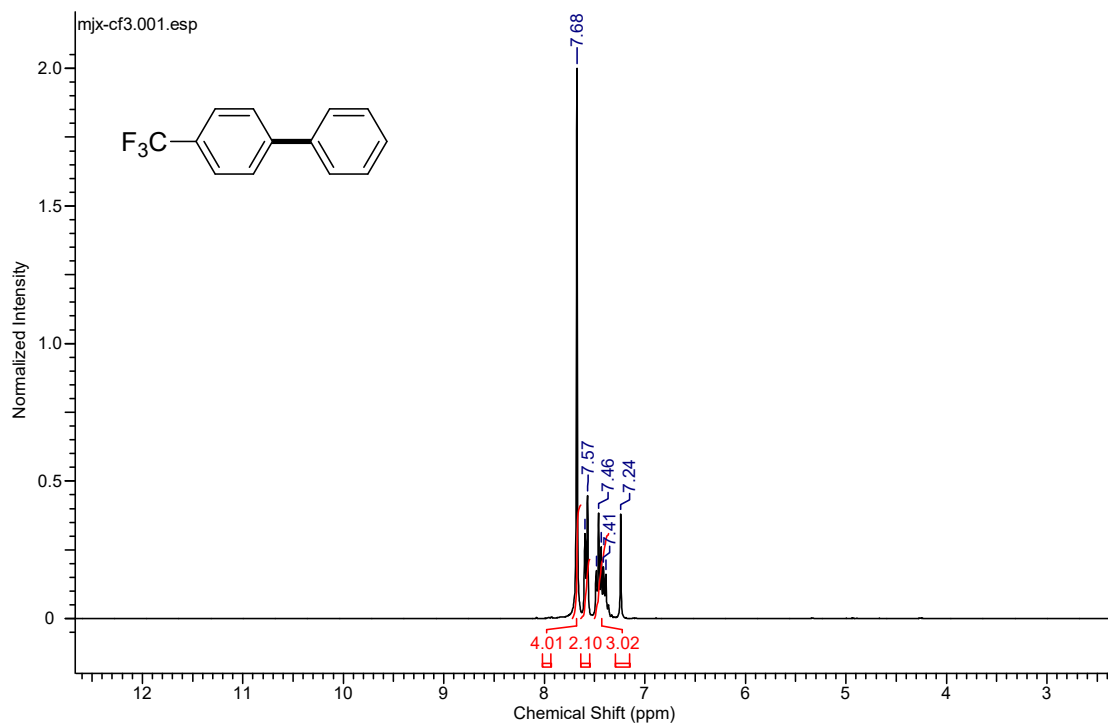


Figure S23. ^1H NMR spectrum of 4-(trifluoromethyl)-1,1'-biphenyl (**7**)

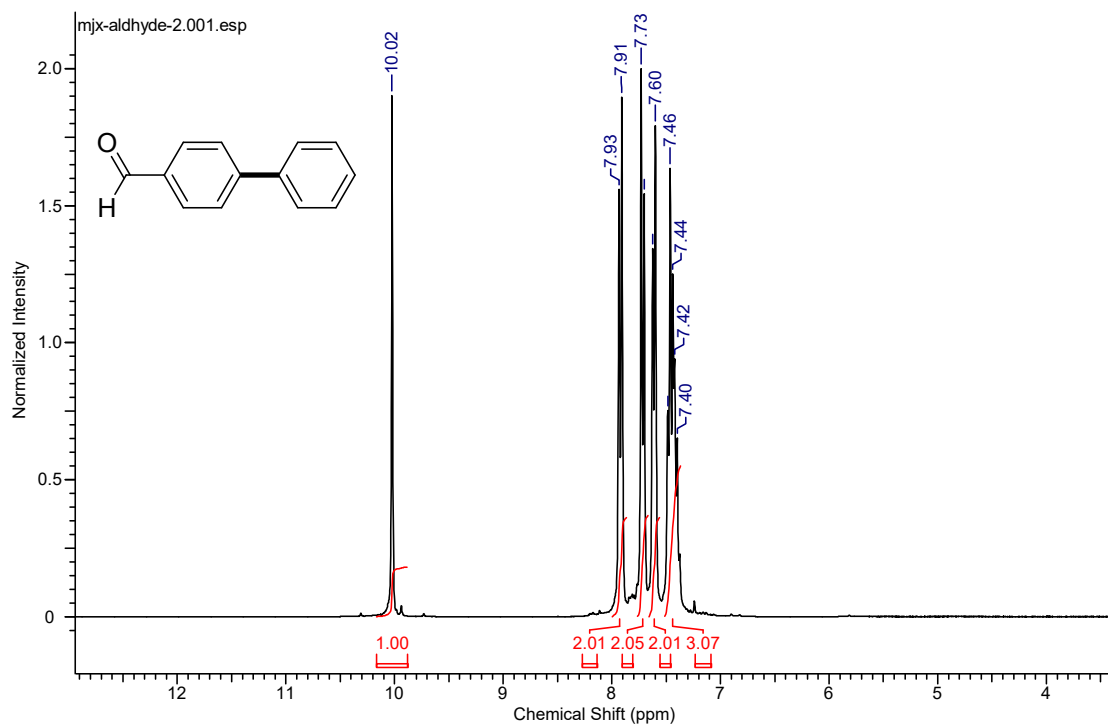


Figure S24. ^1H NMR spectrum of [1,1'-biphenyl]-4-carbaldehyde (**8**)

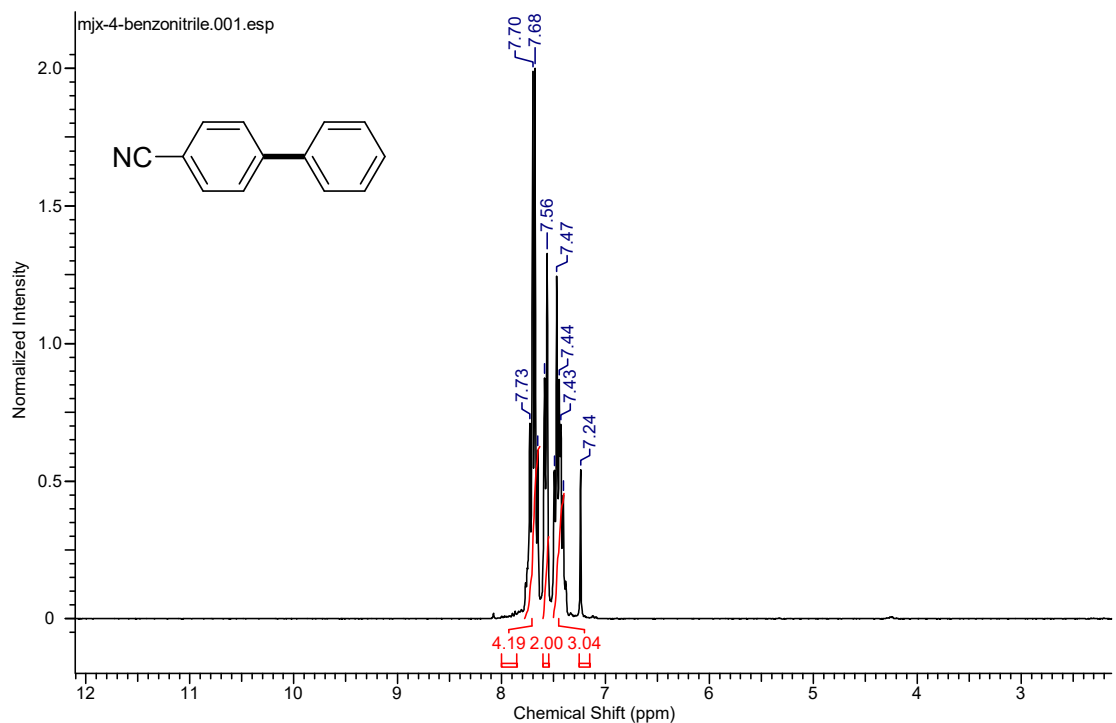


Figure S25. ^1H NMR spectrum of [1,1'-biphenyl]-4-carbonitrile (**9**)

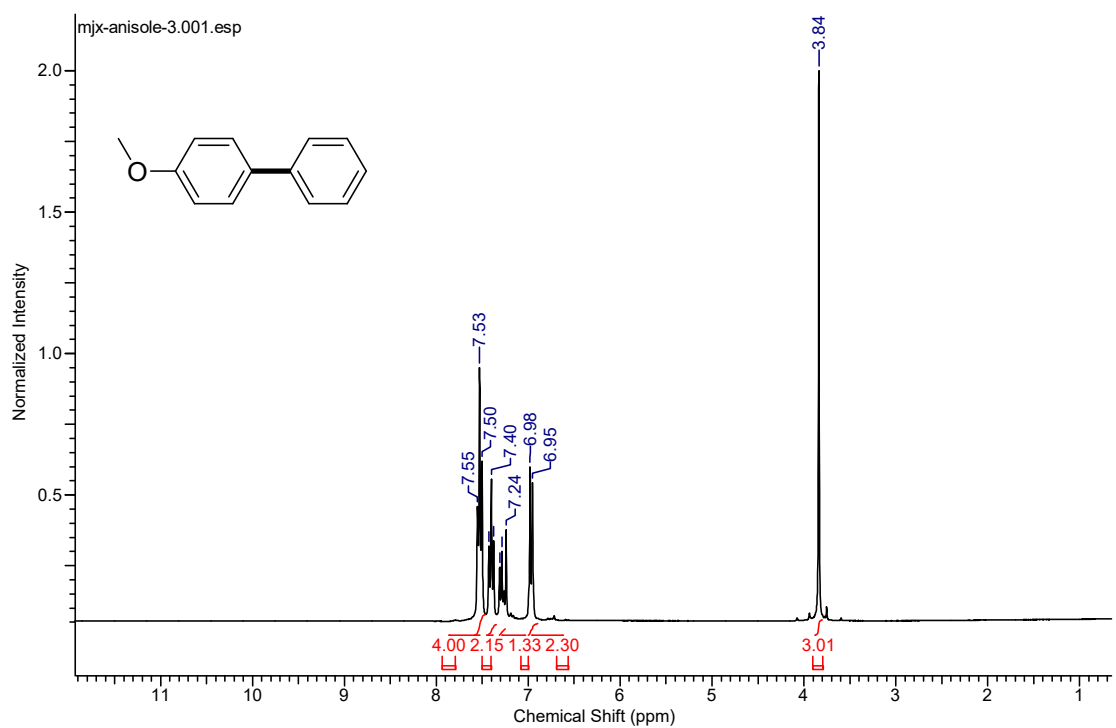


Figure S26. ^1H NMR spectrum of 4-methoxy-1,1'-biphenyl (**10**)

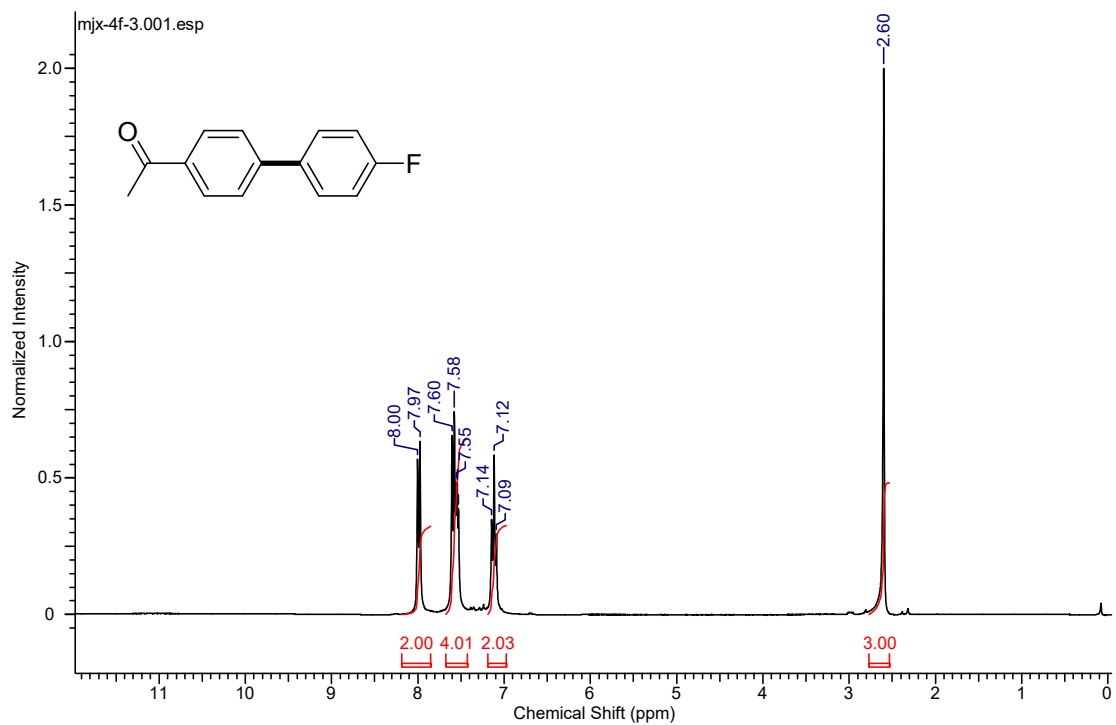


Figure S27. ^1H NMR spectrum of 1-(4'-fluoro-[1,1'-biphenyl]-4-yl)ethanone (**11**)

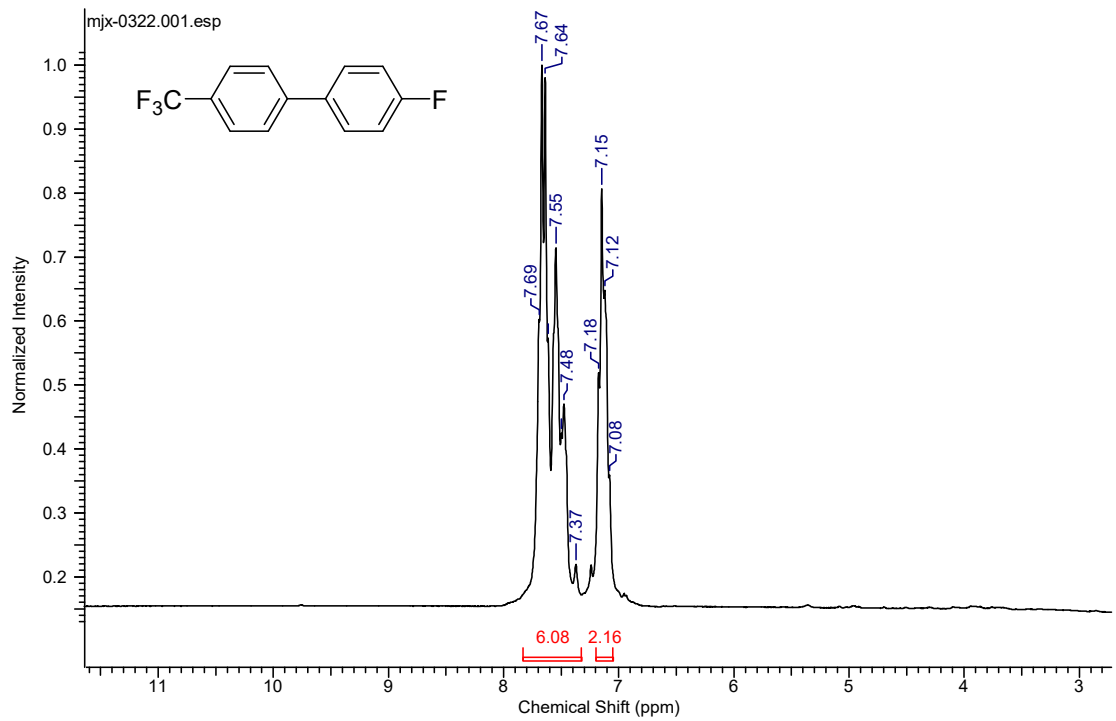


Figure S28. ^1H NMR spectrum of 4-fluoro-4'-(trifluoromethyl)-1,1'-biphenyl (**12**)

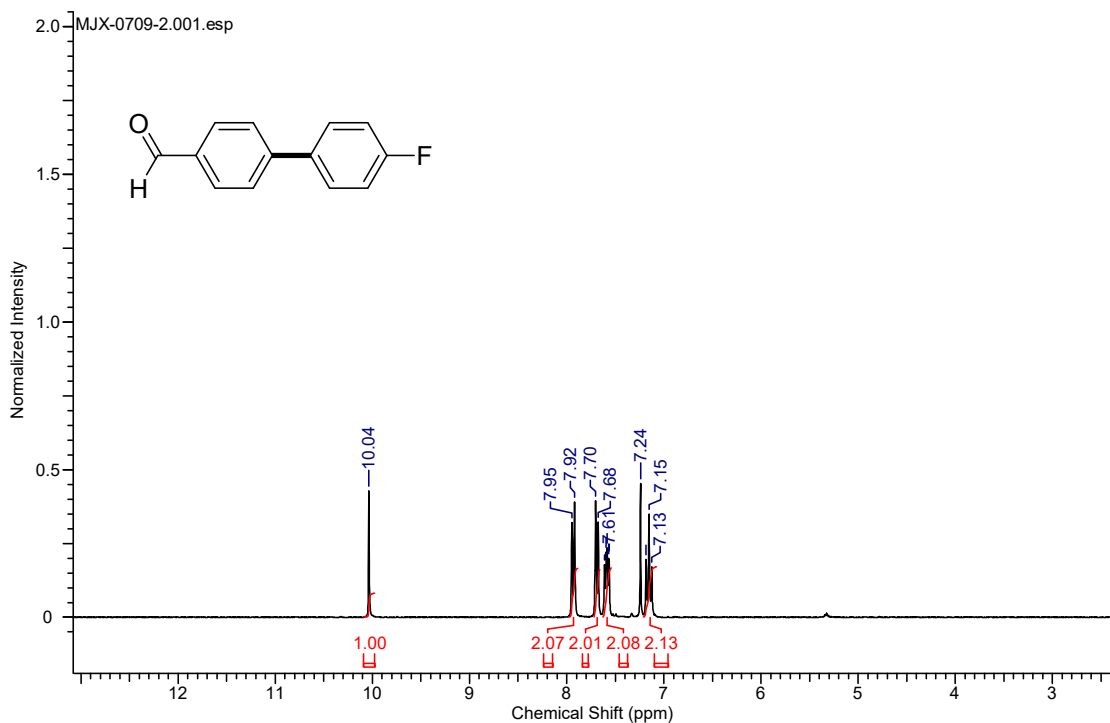


Figure S29. ^1H NMR spectrum of 4'-fluoro-[1,1'-biphenyl]-4-carbaldehyde (**13**)

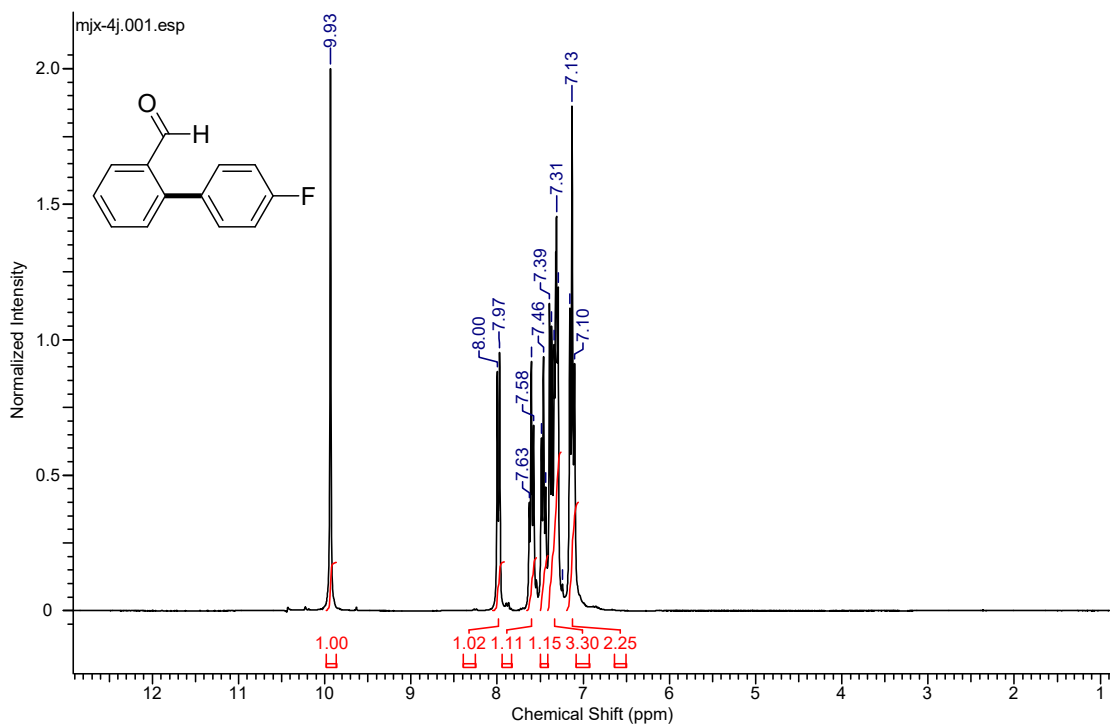


Figure S30. ^1H NMR spectrum of 4'-fluoro-[1,1'-biphenyl]-2-carbaldehyde (**13'**)

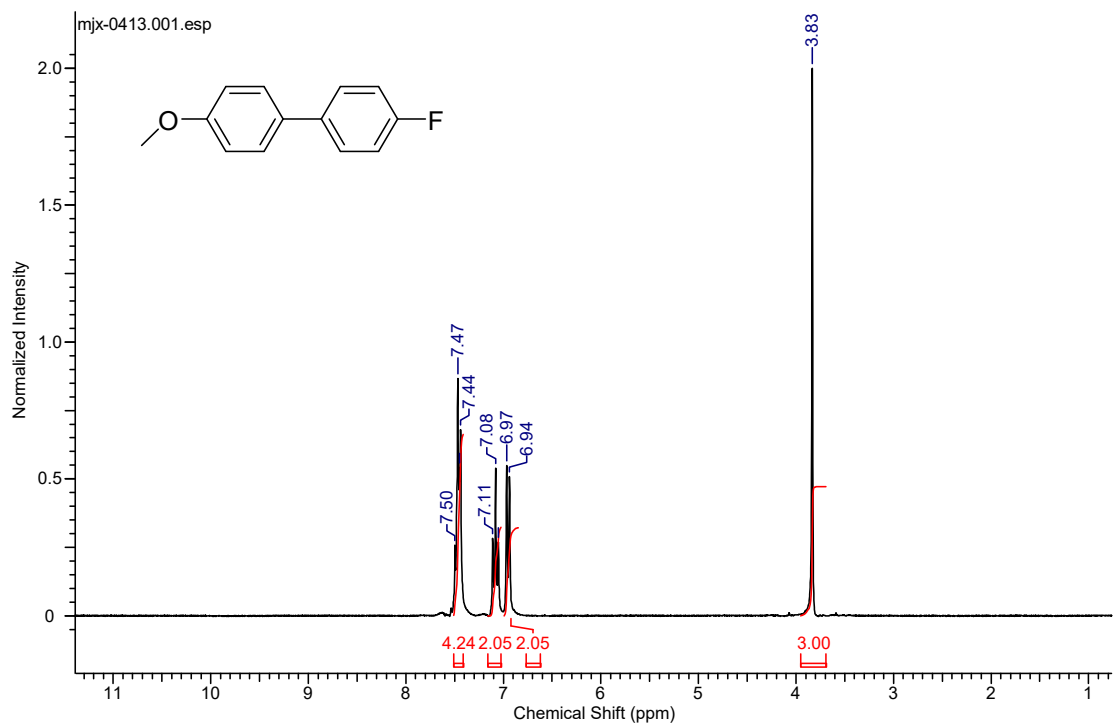


Figure S31. ^1H NMR spectrum of 4-Fluoro-4'-methoxybiphenyl (**14**)

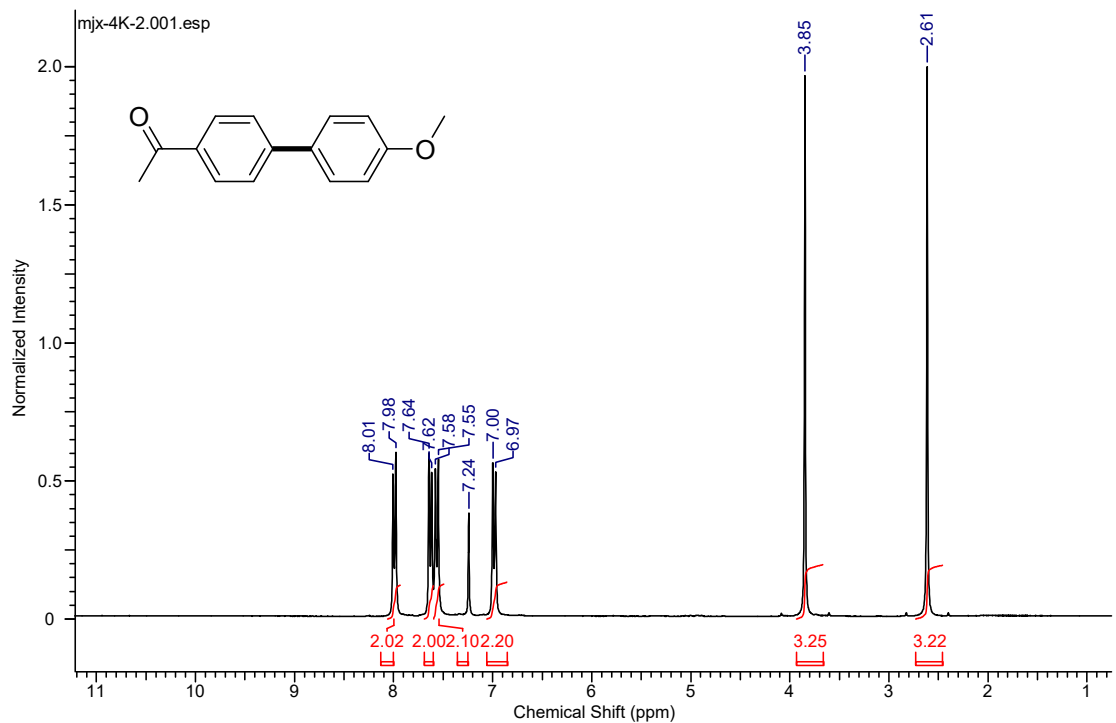


Figure S32. ^1H NMR spectrum of 1-(4'-methoxy-[1,1'-biphenyl]-4-yl)ethanone (**15**)

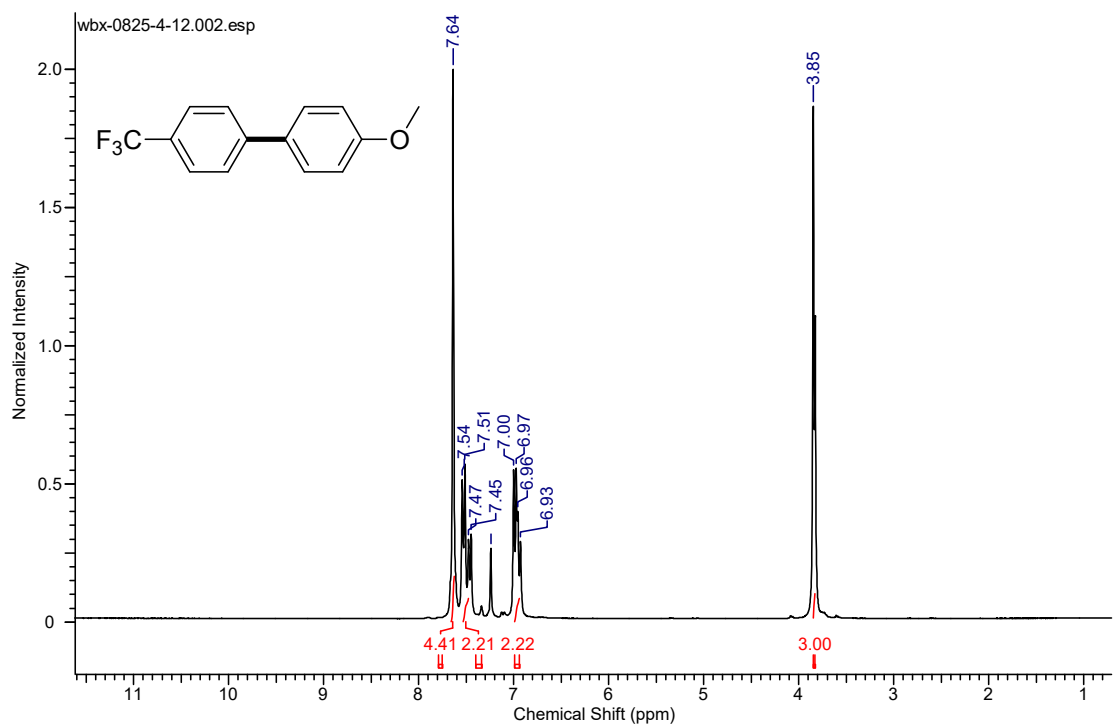


Figure S33. ^1H NMR spectrum of 4-methoxy-4'-(trifluoromethyl)-1,1'-biphenyl (**16**)

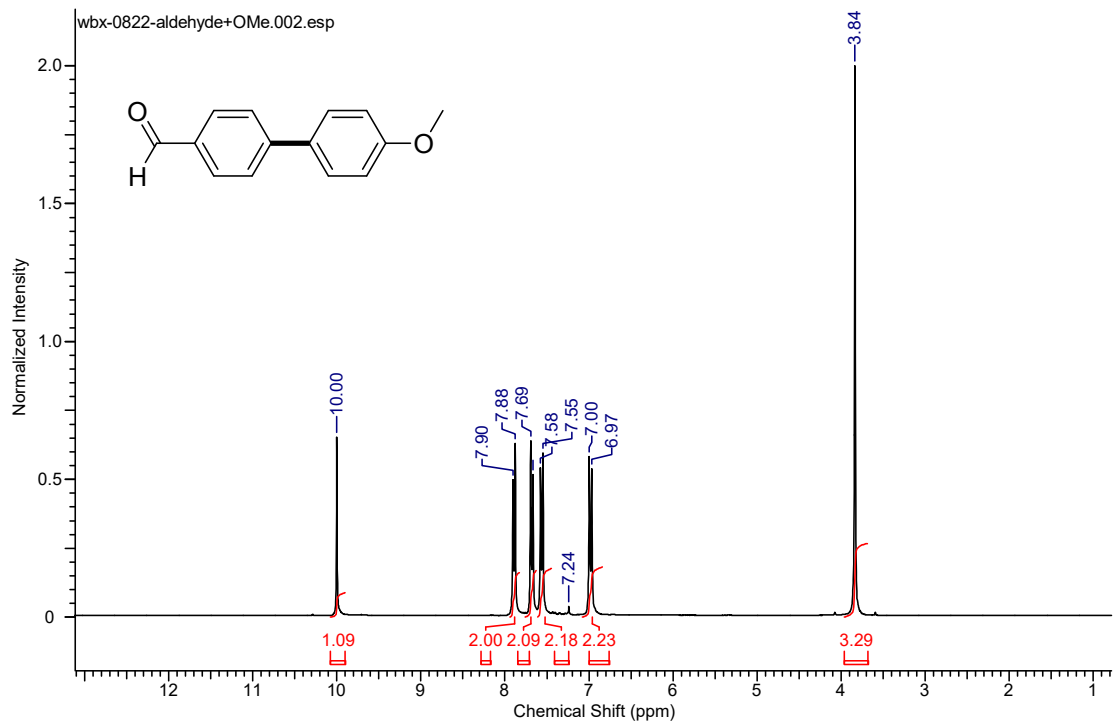


Figure S34. ^1H NMR spectrum of 4'-methoxy-[1,1'-biphenyl]-4-carbaldehyde (**17**)

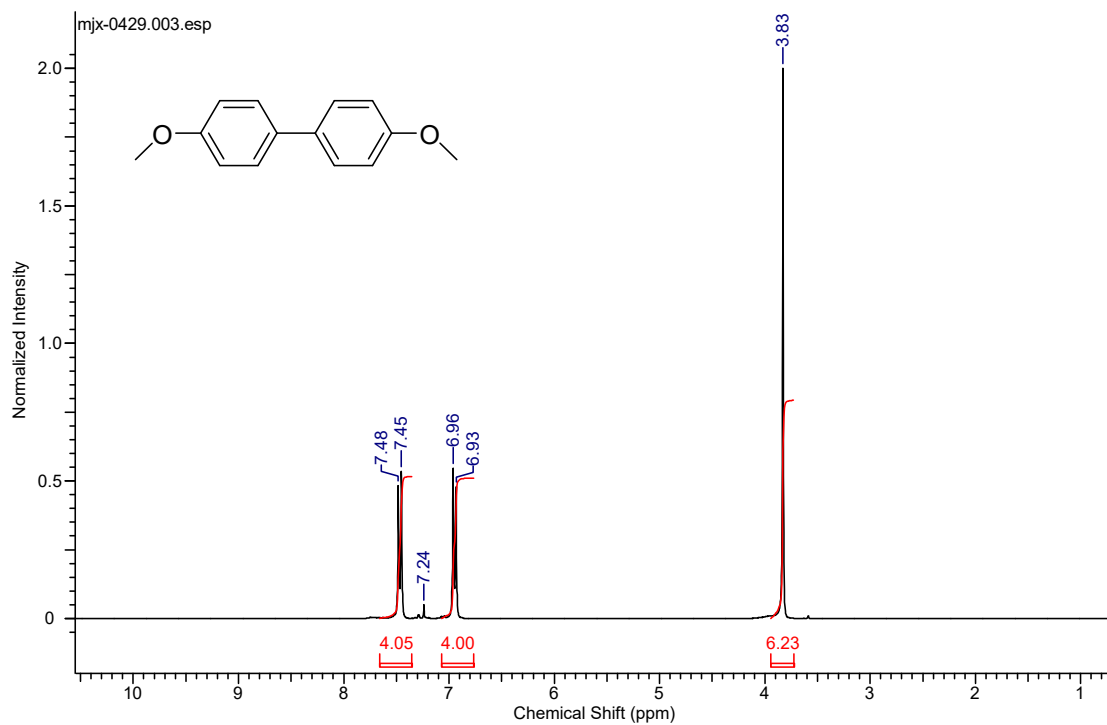


Figure S35. ^1H NMR spectrum of 4,4'-dimethoxy-1,1'-biphenyl (**18**)

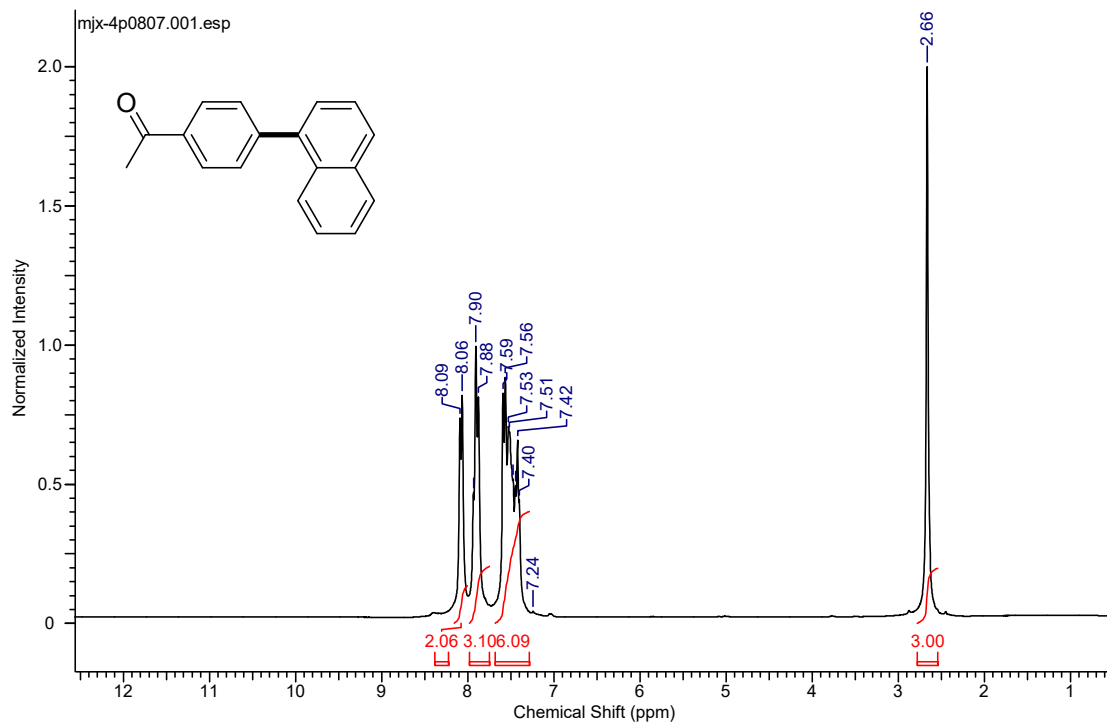


Figure S36. ^1H NMR spectrum of 1-(4-(naphthalen-1-yl)phenyl)ethanone (**19**)

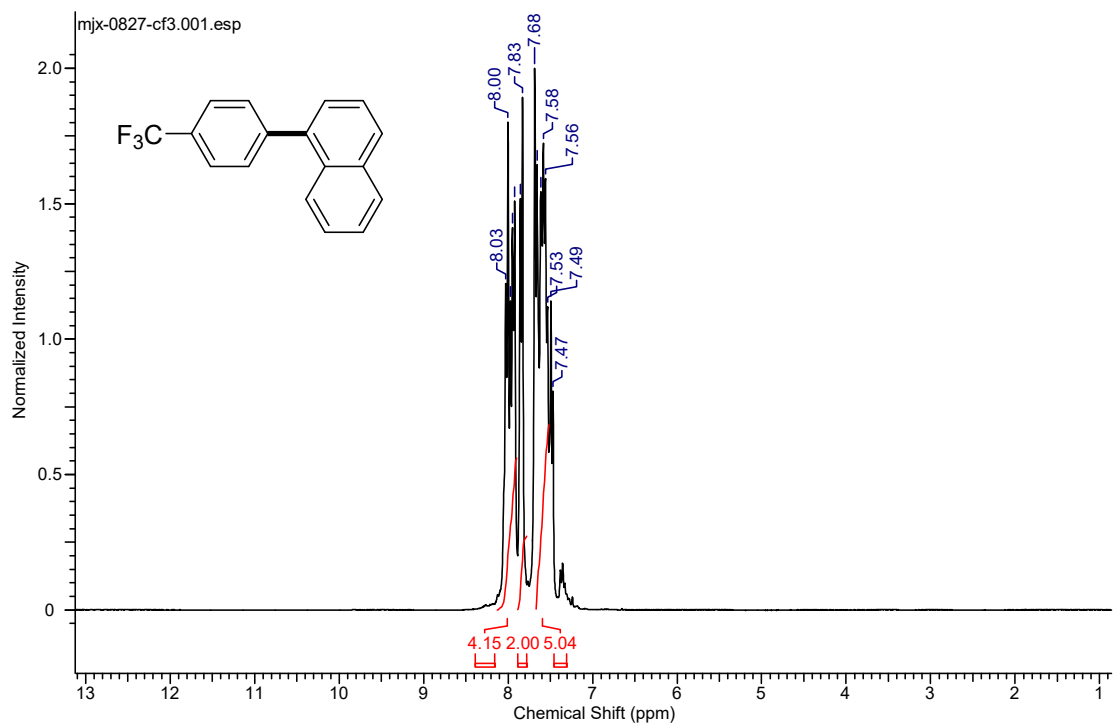


Figure S37. ^1H NMR spectrum of 1-(4-(trifluoromethyl)phenyl)naphthalene (**20**)

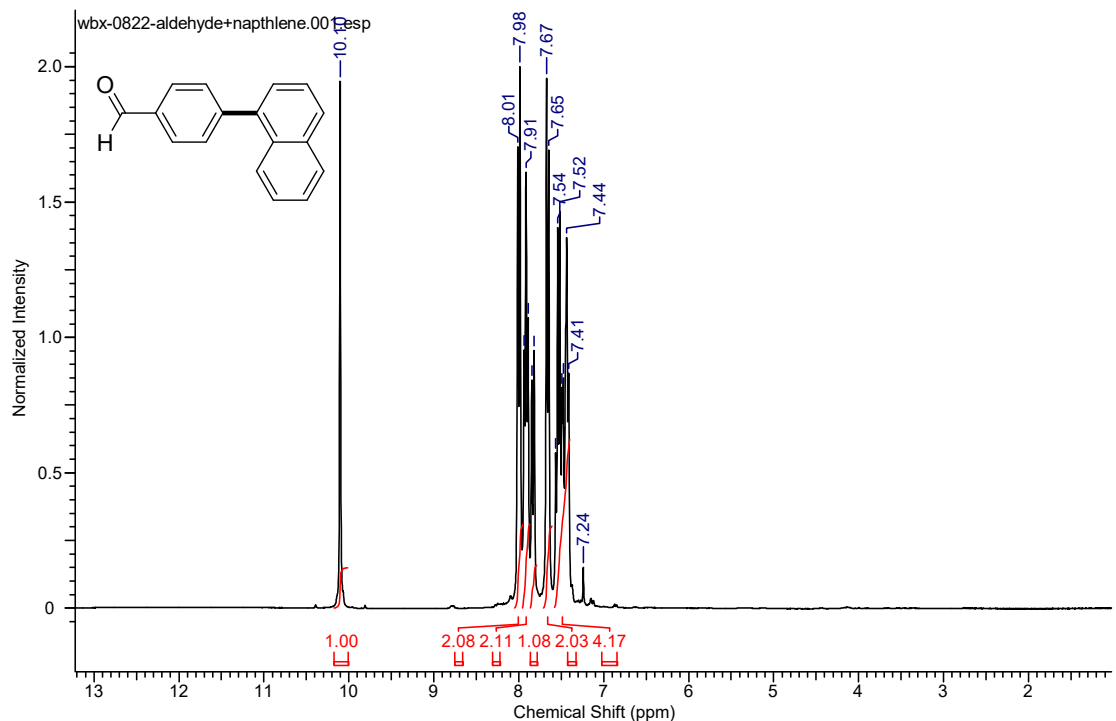


Figure S38. ^1H NMR spectrum of 4-(naphthalen-1-yl)benzaldehyde (**21**)

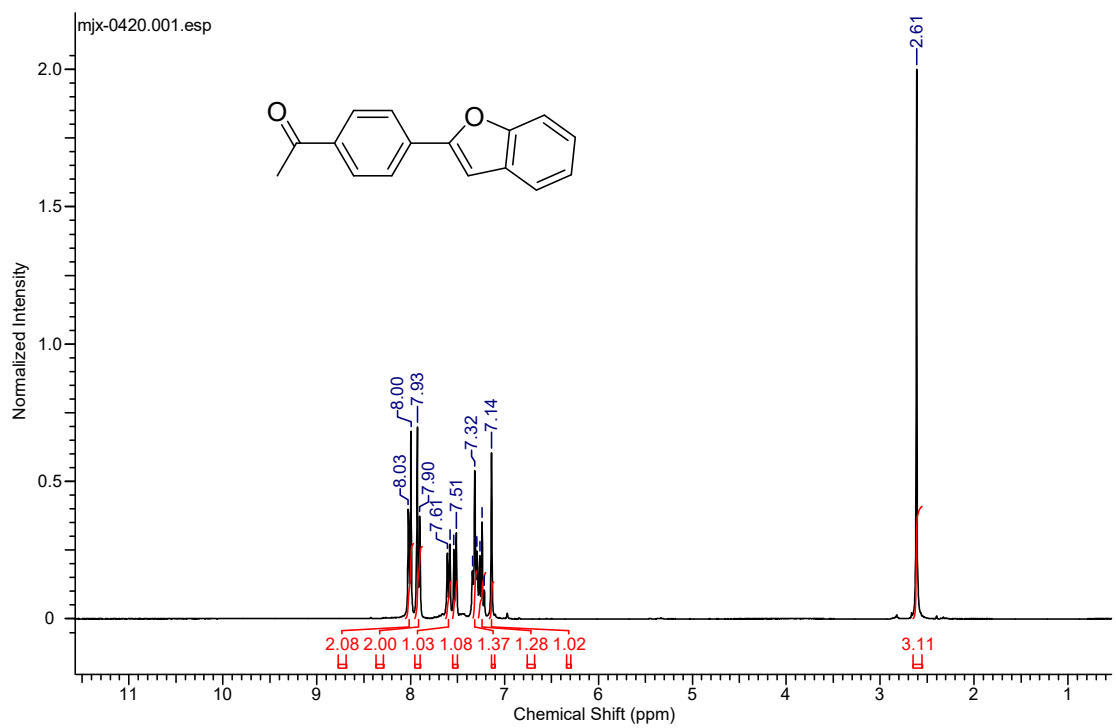


Figure S39. ^1H NMR spectrum of 1-[4-(1-benzofuran-2-yl)phenyl]ethanone (**23**)

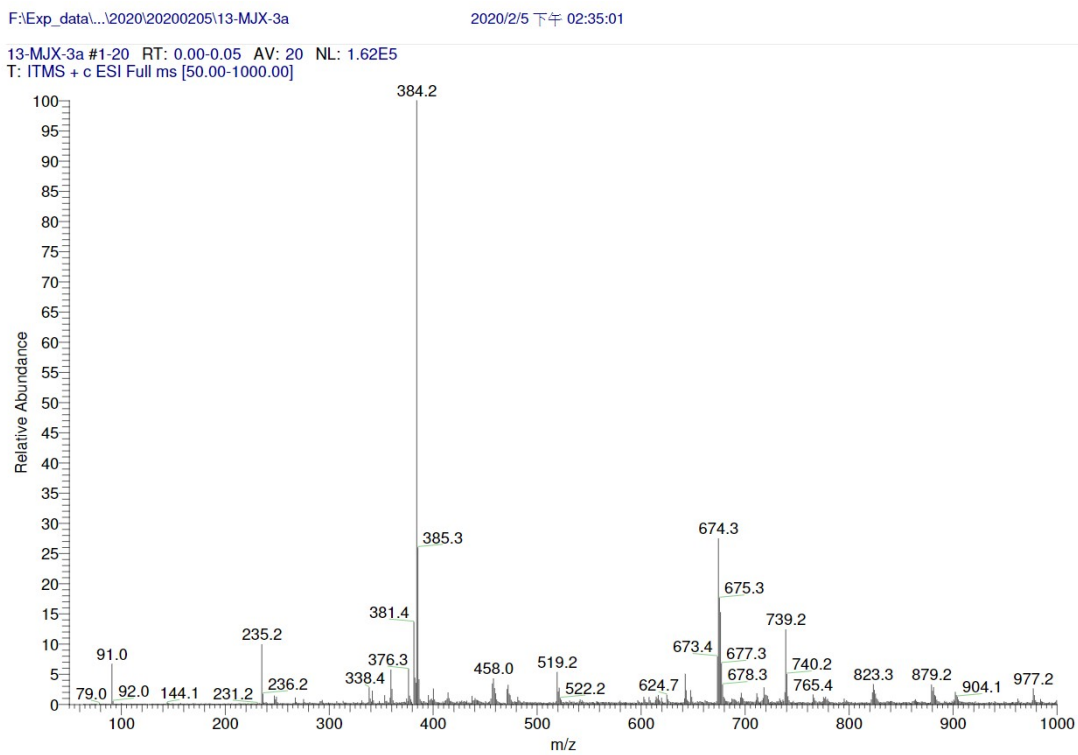


Figure S40. Mass spectrum of complex **3a**.

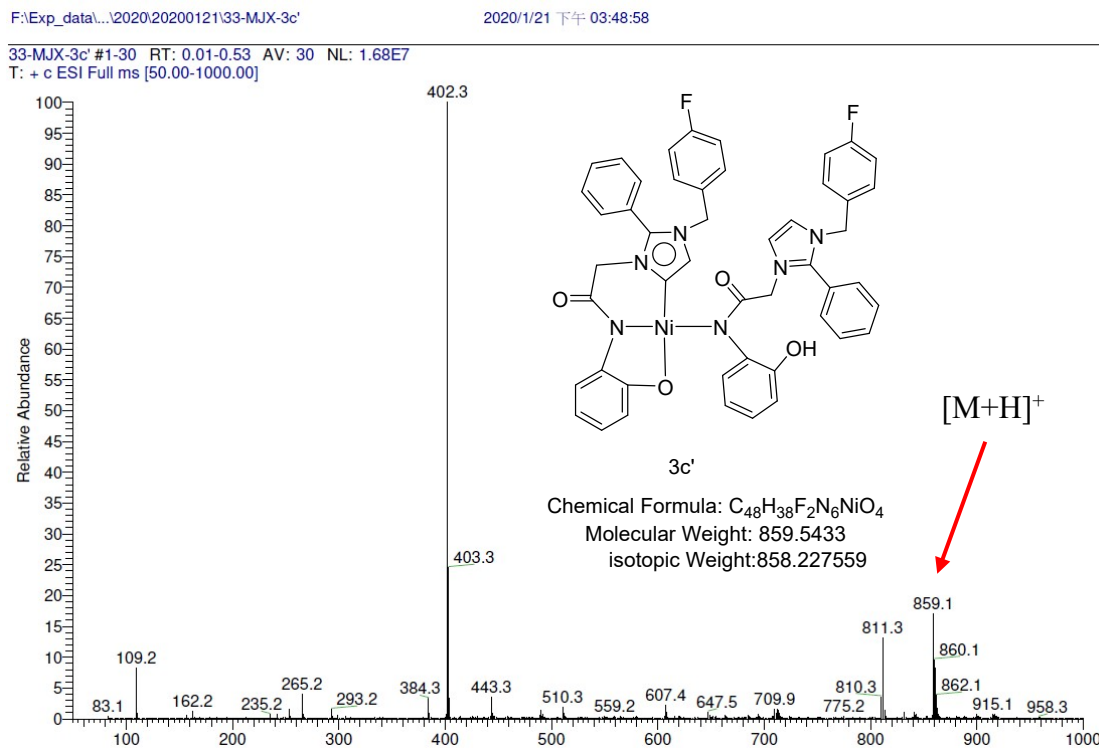


Figure S41. Mass spectrum of complex 3c'.

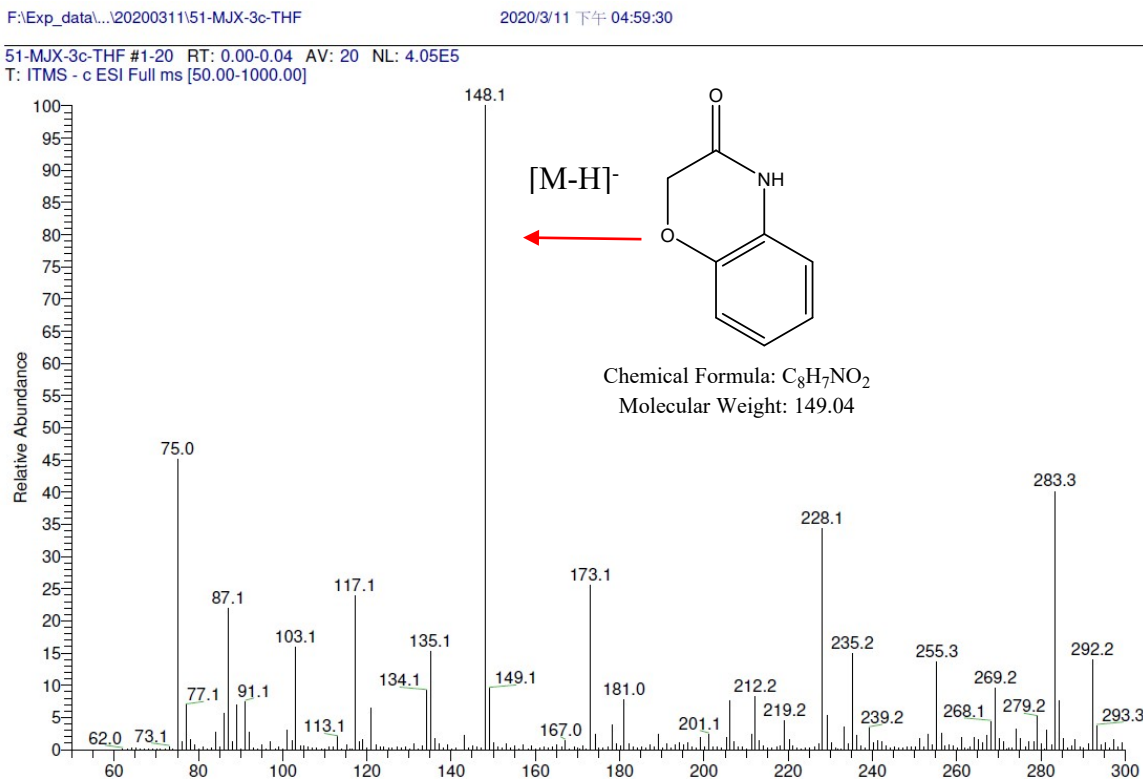


Figure S42. Mass spectrum of complex 5.

References

1. Bruker *APEX and SAINT*, Bruker AXS Inc., Madison, Wisconsin, USA.: 2012.
2. Sheldrick, G. M. *SADABS*, University of Göttingen, Germany: 2003.
3. Sheldrick, G. *SHELXL*, University of Göttingen, Germany: 2015.
4. Spek, A. L., PLATON SQUEEZE. *Acta Crystallogr.* **2015**, *C71*, 9-18.
5. Jiang, Z.-J.; Li, Z.-H.; Yu, J.-B.; Su, W.-K., Liquid-Assisted Grinding Accelerating: Suzuki–Miyaura Reaction of Aryl Chlorides under High-Speed Ball-Milling Conditions. *J. Org. Chem.* **2016**, *81* (20), 10049-10055.
6. West, M. J.; Watson, A. J. B., Ni vs. Pd in Suzuki–Miyaura sp²–sp² cross-coupling: a head-to-head study in a comparable precatalyst/ligand system. *Org. Biomol. Chem.* **2019**, *17* (20), 5055-5059.
7. Ackermann, L.; Potukuchi, H. K.; Althammer, A.; Born, R.; Mayer, P., Tetra-ortho-Substituted Biaryls through Palladium-Catalyzed Suzuki–Miyaura Couplings with a Diaminochlorophosphine Ligand. *Org. Lett.* **2010**, *12* (5), 1004-1007.
8. Delaney, C. P.; Kassel, V. M.; Denmark, S. E., Potassium Trimethylsilanolate Enables Rapid, Homogeneous Suzuki–Miyaura Cross-Coupling of Boronic Esters. *ACS Catal.* **2020**, *10* (1), 73-80.
9. Wang, D.; Zhao, J.; Chen, J.; Xu, Q.; Li, H., Intramolecular Arylative Ring Opening of Donor-Acceptor Cyclopropanes in the Presence of Triflic Acid: Synthesis of 9*H*-Fluorenes and 9,10-Dihydrophenanthrenes. *Asian J. Org. Chem.* **2019**, *8* (11), 2032-2036.
10. Nirmala, M.; Arruri, S.; Vaddamanu, M.; Karupnaswamy, R.; Mannarsamy, M.; Adinarayana, M.; Ganesan, P., Highly active homoleptic nickel(II) bis-*N*-heterocyclic carbene catalyst for Suzuki–Miyaura and Heck cross-coupling reactions. *Polyhedron* **2019**, *158*, 125-134.
11. Zhou, Y.-B.; Li, C.-Y.; Lin, M.; Ding, Y.-J.; Zhan, Z.-P., A Polymer-Bound Monodentate-P-Ligated Palladium Complex as a Recyclable Catalyst for the Suzuki–Miyaura Coupling Reaction of Aryl Chlorides. *Adv. Synth. Catal.* **2015**, *357* (11), 2503-2508.
12. Stibingerova, I.; Voltrova, S.; Kocova, S.; Lindale, M.; Srogl, J., Modular Approach to Heterogenous Catalysis. Manipulation of Cross-Coupling Catalyst Activity. *Org. Lett.* **2016**, *18* (2),

312-315.

13. Zhang, L.-M.; Li, H.-Y.; Li, H.-X.; Young, D. J.; Wang, Y.; Lang, J.-P., Palladium(II) Chloride Complexes of N,N'-Disubstituted Imidazole-2-thiones: Syntheses, Structures, and Catalytic Performances in Suzuki–Miyaura and Sonogashira Coupling Reactions. *Inorg. Chem.* **2017**, *56* (18), 11230-11243.